

# Lawrence Berkeley National Laboratory

## Recent Work

### Title

SPARK DAMAGE AND HIGH VOLTAGE BREAKDOWN OF METALS IN VACUUM AT 14 MEGACYCLES (PRELIMINARY REPORT)

### Permalink

<https://escholarship.org/uc/item/9qn3j4h4>

### Authors

Chupp, Warren W.  
Heard, Harry G.

### Publication Date

1952-09-24

DECLASSIFIED

UNIVERSITY OF  
CALIFORNIA

*Radiation  
Laboratory*

TWO-WEEK LOAN COPY

*This is a Library Circulating Copy  
which may be borrowed for two weeks.  
For a personal retention copy, call  
Tech. Info. Division, Ext. 5545*

BERKELEY, CALIFORNIA

UCRL-1962 Rev.  
c. 2

## **DISCLAIMER**

This document was prepared as an account of work sponsored by the United States Government. While this document is believed to contain correct information, neither the United States Government nor any agency thereof, nor the Regents of the University of California, nor any of their employees, makes any warranty, express or implied, or assumes any legal responsibility for the accuracy, completeness, or usefulness of any information, apparatus, product, or process disclosed, or represents that its use would not infringe privately owned rights. Reference herein to any specific commercial product, process, or service by its trade name, trademark, manufacturer, or otherwise, does not necessarily constitute or imply its endorsement, recommendation, or favoring by the United States Government or any agency thereof, or the Regents of the University of California. The views and opinions of authors expressed herein do not necessarily state or reflect those of the United States Government or any agency thereof or the Regents of the University of California.

UNIVERSITY OF CALIFORNIA  
Radiation Laboratory  
Contract No. W-7405-eng-48

SPARK DAMAGE AND HIGH VOLTAGE  
BREAKDOWN OF METALS IN VACUUM AT  $1\frac{1}{2}$  MEGACYCLES  
(PRELIMINARY REPORT)

Warren W. Chupp and Harry G. Heard

January, 1954

Berkeley, California



SPARK DAMAGE AND HIGH VACUUM VOLTAGE  
BREAKDOWN ON METALS IN VACUUM AT 14 MEGACYCLES

Warren W. Chupp and Harry G. Heard

Radiation Laboratory, Department of Physics  
University of California, Berkeley, California

January, 1954

ABSTRACT

This preliminary report compares the spark damage and breakdown voltage of Inconel, E.T.P. copper, D.H.P. copper, tantalum, molybdenum, nickel, C-18 carbon, K-Monel, stainless steel and satin chrome-plated copper. The tests were made in an oil pumped rf cavity. Breakdown voltages are quoted for tests made with a 15,000 gauss magnetic field in a cylinder opposite parallel-plane geometry. The peak energy storage of the 14 megacycle/<sup>cavity</sup> is approximately 10 joules. A discussion of pertinent observations is included.

SPARK DAMAGE AND HIGH VOLTAGE  
BREAKDOWN OF METALS IN VACUUM AT 14 MEGACYCLES

Warren W. Chupp and Harry G. Heard

Radiation Laboratory, Department of Physics  
University of California, Berkeley, California

January, 1954

I. INTRODUCTION

This report is concerned with the results of high vacuum breakdown and spark damage tests conducted in a 14 megacycle cavity at approximately one megavolt.

The experiments have been of two types. The first type consisted of accumulative sparking on various metals in the presence of a strong magnetic field. All metals were run with fixed geometry. The primary purpose of the magnetic field was to cause sparking damage. The purpose of this series of experiments was to compare the spark damage incurred by various metals to the damage incurred by copper.

The second type of experiment was devised to determine the breakdown voltage for different metals at different electrode spacings.

II. EXPERIMENTAL SETUP AND MEASUREMENT TECHNIQUE

A. General

The test cavity is shown in Fig. 1. 14 megacycle power is inductively coupled into the cavity from the grounded grid oscillator by means of a  $\frac{\Delta}{4}$  line. Under normal conditions up to 800 KW can be delivered to the cavity. The r-f current densities are estimated to be 50-80 amp./lineal inch at 1 megavolt.

The test geometry is illustrated in Fig. 2. With this cylinder-plane geometry the higher gradient is at the cylinder. The most severe spark damage in general is suffered by the closest side plate. A strong magnetic field (approximately 15,000 gauss) is applied normal to the parallel side plates. The purpose of this field is to intensify and localize the damage by strongly collimating the spark discharges.

Each electrode assembly is given a smooth finish (approximately 30-50 microinches), degreased, detergent washed and then finally rinsed in concentrated HCl followed by tap water and C. P. acetone. The plates and stem are regarded as clean enough if water will flow across the surfaces in a smooth sheet and not form rivulets and droplets.

Each run is conducted with the vacuum in the test chamber better than  $10^{-6}$  mm. Hg. untrapped and  $5 \times 10^{-7}$  mm. Hg. trapped.

The test chamber itself is pumped continuously with two 32 inch oil diffusion pumps each pump being isolated from the main manifold by a refrigerated baffle maintained at  $-40^{\circ}$  C. The main manifold contains a liquid  $N_2$  thimble having approximately  $4\frac{1}{2}$  square feet of surface area.

Pressures are measured and recorded continuously at a point in the cavity remote from the pumps. Both trapped and untrapped gauges are utilized to give a continuous relative measure of condensibles in the system. The trapped gauge pressure is generally about three quarters that of the untrapped pressure.

#### B. Breakdown Voltage Measurement

It has been assumed in these tests that the sparking rate is a good index for measurement of the breakdown voltage.

The breakdown voltage for ideal electrodes will be defined as that voltage at which the sparking rate is infinitely discontinuous and the rate is zero at all voltages less than this value. The criterion of breakdown voltage in the practical case has been that voltage at which a small increment in voltage produces a many fold increase in sparking rate which does not decrease with time. It is observed that the sparking rate is not zero below the breakdown voltage and in fact is time and voltage dependent. Breakdown voltages, as monitored by the sparking rate, have been observed both with and without an external magnetic field.

C. Spark Detection and Monitoring Facilities

Vacuum sparks\* were monitored with a stilbene crystal-photomultiplier combination shown in Fig. 3. The x-ray shielded 1P21 photomultiplier was located approximately ten feet from and in line with the stem electrode. After amplification, the spark signals were used to drive pulsers which provided the voltage levels necessary for reliable spark monitoring.

Electronic facilities were provided to:

- (1) Indicate and record the total number of sparks for each set of electrodes.
- (2) Monitor the sparking rate versus time.

---

\* A spark is here defined as the simultaneous occurrence of an abrupt drop in cavity driving point impedance, the emission of visible light at the surface of the emission of an x-ray photon burst of short duration which has an integrated amplitude that greatly exceeds the background x-ray level due to electron loading.

- (3) Record those sparks which occur during the flat-topped portion of the r-f envelope.
- (4) Record the time average distribution of sparks during r-f pulses.
- (5) Record the time distribution of a given spark sequence.
- (6) Measure the time the r-f is applied to the electrodes.
- (7) Oscilloscope monitor and calibrate cavity power input and r-f voltage across the gap.
- (8) Continuously record the integrated x-ray background, and the trapped and untrapped cavity pressures.

#### D. Duty Cycle

During the first two runs of the sparking damage phase of these measurements, the system was operated cw. Continual loss of operating time due to oscillator "outage" required the change to pulsed operation at high levels. The selection of duty cycle and pulse length was based on rough observations of the effect of pulse recurrence frequency and pulse length on the sparking rate. A 176 millisecond pulse with a recurrence rate of 90 or 180 per minute was selected. The lower repetition rate was used where excessive heating occurred from electron loading and low heat conduction.

#### E. Voltage Conditioning

The electrodes were voltage conditioned, that is baked-in, by raising the voltage from approximately 400 kv in steps of 25 to 100 kv in the absence of magnetic field. The magnitude of a voltage increment was determined from the previous sparking rate and its rate of decay. All electrodes were voltage conditioned to 750 kv or better before turning

on the magnetic field. Sparking measurements with the magnetic field generally started around 500 kv and continued until operation was limited by oscillator plate voltage or the breakdown threshold had been reached.

### III. EXPERIMENTAL RESULTS

#### A. Copper

Using the 5-3/8 inch gap geometry several types of copper have been tested to approximately one million volts. The various samples tested were E.T.P., O.F.H.C., and D.H.P. coppers. The D.H.P. was tested with both surface hardened and fully annealed.

Under the test conditions available, sparking at one megavolt does not produce any macroscopic damage to the electrode surfaces provided the magnetic field is not present. Direct observation of these sparks shows that they appear as scintillations occurring randomly over the tip of the center electrode.

The application of the magnetic field (4,000-15,000 gauss) produces a marked change in the anode surface appearance as a result of sparking. Considerable amounts of metal are removed from the nearer side plate and transferred in quantity to the stem and opposite side plate (see Figs. 5, 6, 7, and 8). The damage is severe in that the craters are deep and show evidence of melting. In some cases the spark damage is so locally confined as to erode through 1/8 inch of copper. This is illustrated in Fig. 9.

There are several conclusions to be drawn from the test data plotted in Fig. 4.

(1) Phosphorous deoxidized copper (D.H.P.) appears as the worst choice of coppers for high voltage electrodes. Although no characteristic

breakdown voltage was observed, the sparking rates were so high and the damage incurred so severe as to preclude its use in practical high voltage, high gradient, applications.

(2) As noted elsewhere the sparking rate exhibits a steady decrease in time when the voltage is below the breakdown voltage. Phosphorous deoxidized copper is somewhat of an exception to this rule in that sparking flurries are frequently encountered. At a time when the rate should be decreasing in accord with previous experience, the rate would, for a reason which could not be interpreted in terms of observed variables, abruptly increase by as much as an order of magnitude and then decay again in the characteristic fashion. The phosphorous deoxidized copper plots in Fig. 4 represent the rates including the flurries. Both O.F.H.C. and electrolytic tough pitch copper experienced sparking flurries but only at the maximum voltage and were of short time duration.

(3) Photographs of typical electrodes are included in the appendix which show that generally more severe damage is suffered by the closer side plate (NORTH). These depict quite clearly the mass of metal blasted off this surface and deposited on the stem and opposite plate.

(4) Observations of the time variation of background x-rays\* from electron loading indicate the following:

---

\* Background x-rays were metered by an integrating electrometer whose constants were chosen so that spark x-rays would make a negligible contribution to the recorded level. This choice of slow response time precludes measurement of x-ray loading near the breakdown voltage.

- (a) There is a general decrease of x-ray loading with r-f operating time at a given voltage.
- (b) The rates of decay of x-rays and sparking rate are different.
- (c) The reduction in indicated x-ray level when the magnetic field is applied is due to the location of the ion chamber in relation to the electric and magnetic fields.

(5) The difference between curves (1) and (3) in Fig. 4 represent the sparking rate difference between hard and soft phosphorous deoxidized copper. As noted under (2) of this section, these two curves represent sparking rates observed as a result of flurries; hence, the distinctive difference between the two curves is a measure of the tendency of the material to spark down at a rapid rate for some short period of time.

The threshold for encountering the sparking flurries is that voltage at which the electrodes will spark at a low but finite rate. As the voltage approaches the breakdown value the sparking rate variations will be greater and more frequent. For a given material the harder the surface the lower the sparking rate at a particular voltage (see Figs. 10 and 11). The copper of curve (1) had a nominal surface hardness of Rockwell B26 while the copper of curve (2) measured Rockwell B90. The hardness of standard stock ran from Rockwell B30 to Rockwell B35.

#### B. Tantalum

Tantalum is the only metal which absorbs large volumes of gas included in this series of tests. It was not considered surprising that high sparking rates were obtained with this highly gas sensitive material.



If there exists a direct correlation between sparking rate and outgassing it has not been experimentally verified.

The spark damaged is illustrated in Figs. 12 and 13.

The breakdown voltage for tantalum in the 5-7/16 inch gap geometry was 920 kv.

### C. Molybdenum

Stock molybdenum was run in the 5-3/4 inch gap geometry. Although the maximum applied was 1.10 megavolts the breakdown voltage was not reached.

The sparking rate decayed monotonically at each voltage until one megavolt was reached. At one megavolt the rate of sparking increased from a normal low value of 5 per minute to approximately 200 per minute and the plates were heated to a dull red. When the voltage was increased to 1.10 megavolts the plates heated further until they were orange colored and the sparking rate increased to 345 per minute.

The conclusions reached were:

- (1) The voltage breakdown for this gap is greater than 1.10 megavolts.
- (2) The sparking rate is temperature dependent above 1.0 megavolt.

- (3) Resistance to damage from sparking is good (see Figs. 14 and 15)..

It may be remarked in reference to conclusion (2) that molybdenum evolves considerable amounts of gas at elevated temperatures which may account for the dependence of the sparking rate on temperature.

Previously undegassed molybdenum will evolve CO above 1000° C and N<sub>2</sub> and above 1200° C. N<sub>2</sub> generally accounts for about 60 percent of the gases evolved. One striking property of molybdenum is that once it is degassed and kept clean it only adsorbs a monolayer of nitrogen<sup>1</sup>.

A comparison of normal and degassed samples may yield an answer as to why the sparking rate is so temperature dependent and if it is due to just the evolution of gases.

#### D. Inconel

In terms of spark damage and breakdown voltage Inconel is superior to any of the coppers tested in these experiments. Tests were made with the 1-3/8, 2-3/8, 3-3/8 and 5-3/8 gap geometries. The breakdown voltages for these respective gap spacings were 635 kv, 940 kv, 1065 kv and greater than 1100 kv.

Spark craters and spark damage can be compared with coppers for the 5-3/8 inch gap. Inspection of the electrodes (see Figs. 16 and 17) shows the spark craters to be smaller and less numerous than found with any of the coppers for the same voltage.

Inconel was found to be much less subject to sparking flurries than any of the coppers. The metallic dust from sparks is non-magnetic.

E. K-Monel

The breakdown voltage was never reached with K-Monel electrodes. It can only be said that the breakdown voltage for this material exceeds one megavolt for a 5-3/8 inch spacing.

The spark craters and total spark damage compare in size and extent to the observed with Inconel for the same geometry (see Fig. 18).

Metallic dust which accumulated on the center electrode during sparking was found to be very magnetic. Heating from r-f skin loss and electron loading apparently altered the structure of the side electrodes as they were found to be magnetic after the test.

It has been hypothesized that the presence of magnetic dust particles will complicate the sparking problem by forming spicules on the surface of the electrodes in the direction of the magnetic field. There has been no direct experimental verification of this phenomenon.

F. Graphite

Graphite electrodes were previously tested by Baker and Birge in the XC cavity using a nominal 7 inch gap geometry. Under their test conditions it was found that electron loading was severe (e.g. it required 1500 kw input to reach 700 kv) and that extreme heating at the r-f contacts was present.

A run has been made using a 1 inch gap to provide high gradient at low voltage. The r-f contacts were provided by the following method:

(1) Copper was sprayed on the surface of the graphite along the edge where contact was to be made in a ribbon about 1 inch wide. An effort was made to make the sprayed metal as thick as possible without

peeling. A coating about 30 mils thick was applied.

(2) A copper sheet was lapped partly over the sprayed region and heliarc welded in place. The electrode assemblies are shown in Figs. 19, 20, and 21.

The observations made were as follows:

(1) The power loss in the cavity was closely proportional to the square of the voltage in the range from 150 kv to 300 kv which was the total range of voltages applied (see Fig. 22).

It was not possible to determine directly the power loss in the carbon electrodes although the losses were certainly large and heating in the gap was clearly evident. At 300 kv an area about 6 inches in diameter was glowing red on the side plates opposite the tip of the stem (at the point where the r-f current node exists).

It should be remarked however, that with comparable oscillator efficiency 500 kv can be reached at 171 kw with Inconel plates but it required 203 kw to reach 310 kv in the graphite run. It required 82.5 kw to reach 292 kv and 156 kw for 530 kv in the case of electrolytic copper. There is then approximately 50 percent of the power loss that is not accountable as cavity losses.

(2) The sparking rate observed at a given voltage for all materials previously tested decays with time at the lower voltages (bake-in effect), this is also true of graphite. If, however, the voltage is turned off for some few minutes the sparking rate returns to its previous high value. This is just the inverse of what has been observed with the other metals tested. The graphite was run over a range of duty cycles ranging from 0.176 to 1.0 with no change in this effect.

(3) In order to minimize the effects of outgassing on sparking rate behaviour, a C. W. run was made wherein the voltage was pushed always to <sup>begin to</sup> the point where sparking would/cut down the duty cycle. A voltage maximum of 310 kv was reached and the sparking rate decayed from 1610 per minute down to 720 per minute.

This value of voltage does not represent a breakdown value but was the maximum voltage that could be reached with a reasonable expenditure of effort and thus may be called a practical voltage limit.

(4) Outgassing is always present and correlates with an increased sparking rate.

Viscious sparks were observed to ~~pass between the~~ electrodes. If these caused damage to the electrodes it was of the order of the granularity of the graphite.

The qualitative observations made on this run indicate that high sparking rates are to be expected but they decrease approximately 25 percent per minute of voltage/<sup>on</sup>time. If the voltage goes off even for a short period the sparking rate will increase to the initial value.

All these remarks are applicable only to this particular test of untreated stock grade C-18 graphite in the XC cavity.

In conclusion it must be said that graphite behaves in an anomalous fashion compared to all other materials tested and that the data does not exist to state what fraction of the cavity power losses were skin losses and what fraction was loss due to electron loading.

#### G. Nickel

A test with nickel in the 5-3/8 inch gap geometry showed that the breakdown voltage for this spacing exceeds one million volts.

After bake-in without field, the magnet was switched on at 15,000 gauss without lowering the r-f voltage. This caused a very high initial sparking rate which decayed in the usual manner.

Inspection of the side plates after approximately 100 minutes of operation at 950 kv show sparking damage similar to K-Monel and Inconel.

As expected for nickel the metallic spark dust was magnetic.

#### H. Stainless Steel (18-8)

Non-magnetic type 316 stainless steel was tested in the 1-3/8 inch gap geometry. At 928 kv without the magnetic field the plates were running dull red and mechanical oscillations of the stem caused a gap variation which approached 50 percent of the gap width. The breakdown voltage was not reached without the magnetic field.

A gap voltage of 810 kv was reached with the magnet on at which time operation was interrupted by a water leak. Approximately 2500 sparks which were concentrated in a four to five square inch area near the end of the stem had eroded through the .062 inch plate and into a cooling water tube (see Fig. 23). Since the sparking rate at 810 kv before the water leak was high and not decaying with time it has been assumed that 810 kv is a representative value for the breakdown voltage.

The metallic dust from the stem electrode was found to be non-magnetic.

#### I. Satin Chrome Plated Copper

A set of E.T.P. copper electrodes was high-temperature plated with

a .005 inch hard chrome plate\*. These electrodes were run in the 5-3/8 inch gap geometry. The breakdown voltage was not reached without the magnetic field. After a few sparks at 750 kv with the magnetic field the chrome plate had been removed and the sparking rate was similar to that found with copper (see Fig. 24).

It may be said in general that in any high voltage application where plating techniques are used that either the bond between the base metal and the plating must be able to resist, or the thickness of the plate must absorb the thermal shock resulting from the concentration of energy in a spark. Most plating techniques will result in large amount of occluded hydrogen which must be removed during bake-in.

Since several attempts to make thick, dense, uniform, high temperature hard-chrome plate have not met with success and since the .005 inch plates are easily damaged by the energetic sparks in this machine it may be concluded that, at the present state of the art, chrome plating does not furnish a satisfactory electrode surface in a high energy-storage cavity.

#### J. Welding and Solder Tests

A series of four tests was conducted to compare the relative sparking damage of heliarc welded and soldered surfaces.

(1) Inconel-Copper Weld: A 1/2 inch Inconel strip was heliarc welded into the center of the phosphorous deoxidized copper side

---

\* The high temperature chrome plate results in less occluded gas to be removed during bake-in. See Brenner, Burkhead and Jennings, Jour. of Res. Bur. of Stds., U. S. Dept. Comm., RP-1854, V-40, Jan. 1948.

plates (see Fig. 25) with number 372 Anaconda rod. The stem electrode for this test was Inconel. It is obvious from the photograph that the sparking damage increases going from Inconel to the weld to the phosphorous deoxidized copper plates.

(2) Solder Tests: Copper side plates were fabricated with five solder inlays in the area where sparking damage was greatest. Visual inspection of the solder plates after sparking indicated (see Figs. 26, 27, and 28.) that several of the more common solders have poor resistance to sparking damage. On the basis of these tests it is hardly possible to classify the solders other than to say that they rank from good to bad (see Table I). Certainly all of the solders, regardless of whether they were applied by heliarc or torch, are more subject to sparking damage than the copper base. Easy Flo and Sil-Fos showed the greatest sparking damage.

#### IV. DISCUSSION

##### A. Effect of the Magnetic Field On Spark Initiation

The time required for a spark to build up (as monitored by x-rays) is not changed by a strong magnetic field<sup>2</sup>. When the breakdown voltage is reached with the magnetic field and the sparking rate is monitored as the magnet is switched off, the sparking rate shows no immediate change. These observations are interpreted as evidence that the initiating mechanism of the vacuum spark is independent of the magnitude of the externally applied magnetic field.

##### B. Magnetic Field - Distance Relation for Damaging Sparks

There is data which shows that a magnetic field threshold exists for damaging sparks. This threshold is a direct function of the electrode



spacing. For the 1-3/8 inch gap damaging sparks begin to appear at all magnetic fields in excess of 2000 gauss. When the gap is 5-5/16 inches damaging sparks do not appear until the magnetic field exceeds 4000 gauss. The magnetic field threshold for a fixed geometry is a function of the electrode material.

C. Sparks With and Without Magnetic Field

There is a striking difference between sparks which occur with and without the magnetic field. Sparks without the field always appear at the surface of the electrode of highest gradient. The visible ionization from these sparks usually extends approximately one inch from the electrode. Sparks without the magnetic field do not cause macroscopic damage to the electrodes. In one test without the magnetic field more than 10,000 sparks passed between the electrodes of which more than 5,000 occurred while at the breakdown threshold. When the system was opened for inspection no sensible macroscopic damage was found. In an extension of this test highly polished electrodes were sparked approximately 2700 times without the magnetic field at voltages from 500 to 1100 kv. Microscopic examination revealed no sparking damage to the side plates. There were microscopic marks on the stem (highest gradient) which corresponded to the areas where scintillations were observed. Typical photographs at 50 X magnification are Figs. 29 and 30.

If the magnetic field is turned on at low values the spark does not change in appearance. Sparks at full field always cause disruptive discharges of incandescent metal from the electrode of lowest gradient. A spark can tear out several milligrams of metal. The amount of metal removed is roughly proportional to the stored energy of the cavity and is a function of the electrode material.

The charge to mass ratio of the incandescent metal is quite low. Jets of metal are observed to start normal to the surface of origin and proceed in straight lines crossing the electric and magnetic field lines. Though a large amount of the vaporized metal sticks to the high gradient electrode, there is always some metallic dust in the bottom of the cavity at the conclusion of a run. Because the bond between some of the transferred metal and the electrode is mechanical rather than fusile, the surface coat frequently cracks and peels. (see Fig. 31)

D. Effect of Magnetic Field on Breakdown Threshold

A test was performed to isolate and study the effect of the magnetic field on the observed breakdown voltage. In this test the sparking rate was measured as a function of voltage with magnetic field as the parameter. The variation in breakdown voltage with magnetic field is shown qualitatively in Fig. 32 (a) and (b).

It was found that the damaging sparks which occur in the presence of sufficient magnetic field cause the observed breakdown voltage to be lowered. The breakdown voltage is not affected by the magnetic field until the damaging sparks appear; it then drops discontinuously to a lower value. At all values of magnetic field above this the breakdown voltage remains constant at the value found when the damaging sparks first appeared. If the magnetic field is turned off after the sparking threshold has been reached with damaging sparks, there will be no instantaneous decrease in the sparking rate.

On the basis of this test it can only be hypothesized that the theoretical breakdown voltage is the same with and without the magnetic

field if the corresponding voltage could be reached without double-ended damaging sparks. It is reasonable to assume however, that the magnetic field plays no fundamental role but rather that damaging sparks cause such changes in the electrode surfaces as to reduce the observed breakdown voltage. Fortunately, time averaged spark distribution data (to be discussed later) from a previous test on this same material shows that the mean sparking rate is increased approximately 70 percent by the presence of the external field (see Table II). While the mean sparking rate cannot be used to calculate the absolute value of the reduction in breakdown, it does suggest, on the basis of an increased mean sparking rate, that the observed breakdown voltage will be lowered by the external magnetic field.

E. Hysteresis in Breakdown Threshold with Magnetic Field

There appears to be a hysteresis effect in the sparking rate the first time the breakdown threshold is reached with the magnetic field. The sparking rate is always lower the first time the voltage is raised to the breakdown value. This effect is quite pronounced for copper but is almost negligible for materials such as Inconel. The first time the breakdown voltage is reached for copper the sparking rate stays so high that it is necessary to lower the voltage as much as 30 percent before the sparking rate will begin to decay. After copper has once been "broken down" the measured breakdown voltage is lowered 15 to 20 percent. As an example the data for Run 23 on electrolytic copper shows a first breakdown voltage at approximately 700 kv with the 15,000 gauss field. It was necessary to lower the peak voltage to approximately 500 kv (a reduction of 29 percent) before the sparking rate showed the usual decay with time. The breakdown voltage

threshold on the second rise was approximately 550 kv or 21 percent below the voltage measured on the first rise.

Evidence exists to show that a complete recovery to the original breakdown voltage may be effected if the initial damage is not too severe and enough time can be spent on a gradual voltage recovery.

F. Breakdown Voltage Scaling Relation

Early in the sparking damage phase of these measurements it became evident that sparking damage was always concentrated on that side plate which was closest to the stem (see Figs. 33, and 34). In addition it was observed that the breakdown voltage threshold for the same geometry was different for different metals at 14 megacycles. These two facts suggest the existence of a scaling relation between initiation of voltage breakdown and gap spacing. A series of tests were conducted in which the breakdown voltage was measured for three different electrode spacings using Inconel (see Table III). The sparking rate versus voltage curves are shown in Fig. 35. Using a sparking rate of 1000 sparks/min. for comparison these data show the breakdown voltages thresholds to be 635 kv, 940 kv, and 1065 kv for the 1-3/8, 2-3/8 and 3-3/8 inch gaps\*. These test data reveal that the initiation of breakdown voltage scales approximately as

$$V \cong kd^{\frac{1}{2}} \quad k = 110 \pm 10 \quad \text{kv/mm}^{\frac{1}{2}}$$

---

\* The geometry in this cavity is such that wide excursions are permissible in gap spacing before a serious difference in resonant frequency appears. So that differences in gap voltage variation with geometry could be eliminated from the test results, the gap voltage calibration factor was measured for each gap spacing and found to vary less than 5 percent.

It is interesting that the scaling relation for rf breakdown is the same as that previously observed for dc breakdown.<sup>3</sup> Since the value of k in the above relation is in good agreement with that obtained for the dc case, ( $134 \pm 20$  dc) it is possible to select metals for their breakdown properties on the basis of existing data from dc tests.<sup>4</sup> Table IV shows the tested materials classified with respect to values of k.

It is necessary to mention that this rf scaling relation was measured for a 15,000 gauss field which was essentially parallel to the gross electric field between the plates. Since 13 megacycle data has been obtained at low voltages without a magnetic field which fits this relation,<sup>5</sup> it appears that the magnetic field only lowers the measured value of k.

#### G. Effects of Voltage Conditioning on Inconel

An experiment was performed to determine whether or not the reduced sparking rate affected by voltage conditioning was lasting. Electrodes were conditioned by raising the voltage across the electrodes from 584 kv in approximately 50 kv steps to 1025 kv, a value below the breakdown threshold, first without and then with the 15,000 gauss magnetic field (see Fig.36, (a) and (b) for voltage schedule). After the highest voltage had been reached with the field, the voltage was immediately reduced approximately 10 percent to 895 kv and the sparking rate was monitored continuously as a function of time. Bake-in with out field and with field required 220 and 61 minutes respectively.\* In the next 256 minutes at 895 kv only 9 sparks occurred. The rf was then turned off for 8 hours while the system remained under vacuum.

The second day of operation was begun at 975 kv from which the voltage was raised in 102 minutes to the previous peak of 1025 kv. The remaining 485 minutes of operation at the 895 kv level accumulated 11 sparks.

On the third day the start up technique was varied by raising the voltage from 740 kv to the operating value of 895 kv in 70 minutes. The \*Time as here discussed refers to actual rf on time and implies the integrated time during which voltage is applied to the electrodes and is independent of duty cycle, pulse length, etc. The duty cycle was changed from 52.8 percent to 26.4 percent during the third day of this test.

voltage was then held at this value for the remaining 545 minutes of operation during which 19 sparks appeared. After another 8 hour pumping period the electrodes were worked up from 724 kv to 895 kv in 24 minutes. During the remaining 133 minutes of the test only 6 sparks occurred. It is worth mentioning that the observed sparking rate at 895 kv is of the order of the usual background counts obtained from the photomultiplier and spark monitoring circuits.

It is concluded on the basis of this test data that:

- (1) If the electrodes are conditioned to a voltage below the breakdown threshold and are operated at lower than the highest peak voltage reached, there is a permanent reduction in sparking rate.
- (2) The initial bake-in is effective and lasting. During the four consecutive days of operation there was little or no increase in sparking rate as a result of the 8 hour periods when the r-f was turned off.
- (3) If the electrodes are conditioned as mentioned in (1) above, it makes no difference whether the operating voltage is reached by returning first to the highest bake-in voltage or by stopping when the operating voltage is reached.

#### H. X-Ray Loading

- (1) Variation With Voltage: Since x-ray loading at any voltage varies slowly with time, this function will not be accurately

portrayed if point-by-point data were taken during bake-in. If the x-ray versus voltage data are taken during a small enough interval of time, however, the loading is seen to be an exponential function of voltage of the form

$$I = C_1 V \exp. (C_2 V)$$

Figs. 37 and 38 illustrate the general form of this function for silver and O.F.H.C. copper. These data are not corrected for scattering or variation of absorption coefficient with voltage; they represent measurements taken for decreasing voltage after bake-in without the magnetic field. Since the condition of the electrodes was not the same at the time of the measurement the relative x-ray level at a given voltage cannot be compared. It is of interest to note that the slopes of these curves are approximately the same.

(2) Variation With Time: An experiment was performed which separated x-ray loading from sparking. As a result of this experiment it is concluded that sparking and x-ray loading are not related as cause and effect. When the silver electrodes were first brought to 815 kv the indicated x-ray level at the standard location was 80 mr/hr. After 5 minutes of operation when the level was 90 mr/hr. the voltage was lowered to 650 kv for 2 hours. When the voltage was again raised to 815 kv the x-ray level was only 30 mr/hr. Since no sparks occurred during the entire 2 hour run, the difference in electron loading cannot be related to sparking decay<sup>9</sup>.

The difference in electron loading is interpreted as being due to surface degassing of the cavity and in particular the electrode

surfaces. Further evidence that absorbed surface gas affects electron loading comes from two common observations.

- (a) X-ray loading at a given voltage increases if operation at a particular voltage is interrupted for a sufficient period.
- (b) Introduction of a small air leak for a short period reduces the x-ray level by as much as a factor of five.

The fact that the above mentioned phenomena occur on a macroscopic time scale suggests that they may be due to sorbed gas films.

#### I. Variation of Sparking Rate with Temperature

Although the exact formulation for the variation of sparking rate with temperature is not known at present, there is positive evidence in Fig. 39 that this effect exists. This graph shows that the sparking rate of 1000 kv is lower than and only becomes comparable at 1025 kv to that observed at 940 kv. There was a 2 hour interval between the data at 940 kv and at 1000 and 1025 kv. This data correlates with the common observation that sparking rates increase if pre-excitation occurs too soon after the tank is sparked down.

#### J. Microscopic Examination of Inconel Electrodes

Photomicrographs (68 X) were made of the spark craters on the Inconel side plates. Fig. 40 shows a cross section of a typical crater .025 inches in diameter. Radial cracks resulting from stress concentration extend .002 to .008 inches from the crater surface. There is evidence of



extensive surface heating of the electrodes in Fig. 38, where the crystal pattern (Fig. 41) shows an area of recrystallization extending .005 to .007 inches into the surface. Figs. 42 and 43 show fusile and mechanical bonds between the electrode surface and the material transferred by a spark.

V. ACKNOWLEDGMENTS

The personnel who assisted with this work consisted of: R. L. Anderson, R. W. Birge, P. R. Byerly, Jr., J. E. Griffith, C. W. Jenson, E. J. Lofgren, R. M. Richter, J. Riedel, W. W. Salsig, H. L. Smith, H. W. Vogel and others.

REFERENCES

1. S. Dushman, Scientific Foundations of Vacuum Technique, John Wiley and Sons, p-633, (1949).
2. H. Heard, E. Lauer and R. Birge, UCRL-1903, (1952).
3. H. Heard, UCRL-1680 (Unclassified excerpt), p-48, (1952).
4. H. Heard and E. Lauer, UCRL-1774, p-10, (1952).
5. F. Schmidt, RL Report BP-29, Fig. 6, (1946).
6. R. Birge and E. Lauer, UCRL-1680, p-18, Fig. 3b, (1951).
7. M. Dazey, D. Nielsen, R. Robertson and D. Sewell, UCRL-1173, p-140 and 35, (1951).
8. Halpern, Everhart, Rapuano, and Slater, Phys. Rev., v-69, p-688-A, (1946).
9. W. Kilpatrick, UCRL-1903 (Unclassified excerpt), p-3, (1952).

TABLE I

COMPARISON OF SPARK DAMAGE OF SOLDERS

<u>SIDE PLATE ELECTRODE MATERIAL</u>	<u>STEM ELECTRODE MATERIAL</u>	<u>NAME</u>	<u>SOLDER PERCENT COMPOSITION</u>	<u>METHOD OF SOLDER APPLICATION</u>	<u>FLUX USED</u>	<u>RESISTANCE TO SPARKING DAMAGE</u>
E. T. P. Copper*	E. T. P. Copper	BT	72 Ag; 28 Cu	Oxy-Acetylene Torch	Handy Flux	Good
		RE-Mn	65 Ag; 28 Cu; 5 Mn; 2 Ni		Handy Flux	Bad
		RE-Sn	60 Ag; 30 Cu; 10 Sn		Handy Flux	Bad
		Sil Phos	15 Ag; 80 Cu; 5 P		Handy Flux	Bad
		Phos Cu	92 Cu; 8 P		None	Bad
D. H. P. Copper**	O. F. C. H. Copper	*** Allstate 175	75 Ag; 25 Cu	Heliarc	Allstate 200	Good
		Incosil	65 Ag; 25 Cu; 10 In		Handy Flux	Fair
		Wes Go Gold	65 Cu; 35 Au		Borax Glass	Bad
		Easy Flo	50 Ag; 15½ Cu; 18 Cd; 16½ Zn		Handy Flux	Very Bad
		BT	72 Ag; 28 Cu		Handy Flux	Good
D. H. P. Copper	O. F. H. C. Copper	Easy Flo	72 Ag; 28 Cu Zn, Cd and C free	Oxy-Acetylene Torch	Handy Flux	Very Bad
		Wes Go			Handy Flux	Good
		Decarbonized				
		Incosil			Handy Flux	Fair
		Allstate 175			Handy Flux	Good
	BT		Handy Flux	Good		

\* E. T. P. = Electrolytic Tough Pitch

\*\* D. H. P. = Phosphorus De-Oxidized

\*\*\* O. F. C. H. = Oxygen Free High Conductivity

TABLE II

## EFFECT OF MAGNETIC FIELD ON MEAN SPARKING TIME

INCONEL RUN 16

<u>PEAK RF VOLTAGE</u> <u>(KILOVOLTS)</u>	<u>SAMPLING</u> <u>TIME</u> <u>INTERVAL (MIN.)</u>	<u>MAG. (AMPS.)</u>	<u>MEAN</u> <u>SPARKING</u> <u>TIME</u> <u>(MILLISEC.)</u>	<u>SPARKS SAMPLED</u>
845	0-13	0	97.46	449
965	0- 6	0	93.69	499
	0-11	0	95.07	614
	6-11	0	101.08	115
1013	0-10	0	98.81	783
1025	0-11	0	97.00	792
880	0- 8	1000	54.76	263
950	0- 5	1000	55.58	389
	5-10	1000	57.19	223
1025	0- 1	1000	62.86	150
	1- 2	1000	55.30	110
	2- 5	1000	59.36	726
	0- 2	1000	59.22	262
	0- 5	1000	55.61	953
	0-12	1000	40.98	1018
	12-16	1000	62.90	205
1025	0-10	1000	68.95	92

TABLE III

INCONEL TEST OF SCALING RELATION

FREQUENCY 14 MC.

GAP SPACING (mm)	GAP* VOLTAGE (KV)	$k = V/d^{\frac{1}{2}}$ (KV/(mm) <sup>1/2</sup> )
35.0	635	109
60.4	940	120
85.6	1065	116

D. C. TEST DATA

0.2	60	134
-----	----	-----

\* Voltage at which average rate is of the order of 100 sparks per minute.

TABLE IV

## CLASSIFICATION OF METAL BY BREAKDOWN VOLTAGE

AT 14 MC WITH 15,000 GAUSS FIELD

<u>METAL</u>	<u>CLOSEST GAP (MM)</u>	<u>GAP VOLTAGE KV</u>	<u><math>k = V/d^{1/2}</math> (KV/mm<sup>1/2</sup>)</u>	<u>REMARKS</u>
Stainless 316	35	700	118 ± 5	k may be low due to water leak.
Inconel	35 60 86	635 940 1065	109 ± 8 120 ± 8 116 ± 5	
K-Monel	137	1050	>98	Peak voltage limited by oscillator power.
Nickel	135	995	>86	Peak voltage limited by oscillator power.
Molybenum	137 54	1200 750	103 ± 4 102 ± 8	
O. F. H. C. Copper	84	950	103 ± 5	
E. T. P. Copper	60 135	700 1200	91 ± 6 103 ± 4	
Tantalum	138	920	78 ± 5	
D. H. P. Copper Rockwell B <u>90</u>	129	900	79 ± 5	D. H. C. plate surface hardened by shot peening from $R_B$ 27-33 to $R_B$ 89-97
Rockwell B <u>26</u>	131	500	46 ± 2	
Silver	137	775	67 ± 4	
C-18 Carbon	24	310	64 ± 10	Peak voltage limited by oscillator power.

TABLE IV (CONT.)

RELATIVE RESISTANCE OF METALS TO SPARK DAMAGE  
IN THE XC - CAVITY

<u>MATERIAL</u>	<u>TOTAL R. F.</u> <u>ON TIME-MIN.</u>	<u>MAX. TEST</u> <u>VOLTAGE KV</u>	<u>GAP</u> <u>INCHES</u>	<u>PERCENT SPARKS</u> <u>AT MAX VOLTAGE</u>	<u>TOTAL</u> <u>SPARKS</u>	<u>DAMAGE</u>
D. H. P Copper (Shot Peened)	360	1020	5-3/8	63%	18336	Damage to large areas both plates. North plate suffered most damage. One large crater penetrated thru plate.
D. H. P. Copper (Fully Annealed)	121	900	5-3/16	95%	29440	Extensive spark damage to both plates. Spark marks are not restricted to high gradient region.
Tantalum	97	1105	5-7/16	95%	12000	Extensive sparking to both plates and stem. Spark marks 3-5 mm in dia. but shallow.
Satin Chrome Plate	30	750	5-3/8	—	—	Initial sparking removed chrome plate. Sparking continued to exposed copper.
C-18 Carbon	640	310	15/16	—	—	Spark damage if incurred is of the order of the granularity of the C-18 carbon. Low energy sparking.

TABLE V

RELATIVE RESISTANCE OF METALS TO SPARK DAMAGE  
IN THE XC - CAVITY

<u>MATERIAL</u>	<u>TOTAL R. F. ON TIME-MIN.</u>	<u>MAX. TEST VOLTAGE KV</u>	<u>GAP INCHES</u>	<u>PERCENT SPARKS AT MAX VOLTAGE</u>	<u>TOTAL SPARKS</u>	<u>DAMAGE</u>
Molybdenum	988	1100	5-3/8	72%	21728	0.1 - 1 mm dia. craters limited to high field region.
Inconel	238	1085	3-3/8	95%	5666	1-2 mm dia. craters. Spark- ing damage res- tricted to approx. 3 square inch area.
K-Monel	758	1030	5-3/8	90%	14942	Sparsely marked 1-2 mm dia. craters.
Nickel	141	995	5-3/8	95%	9344	Similar to K- Monel and In- conel.
Stainless Steel	243	810	1-3/8	95%	4800	Similar to K- Monel, Inconel and Nickel.
O. F. H. C. Copper	641	1080	5-3/8	89%	6336	Overlaid pat- tern approx. 4 times area of largest sparks on Mo. approx. 1/16 deep.
E. T. P. Copper	335	1250	5-3/8	72%	3200	Similar to O. F. H. C. but deeper craters and more variable in depth.



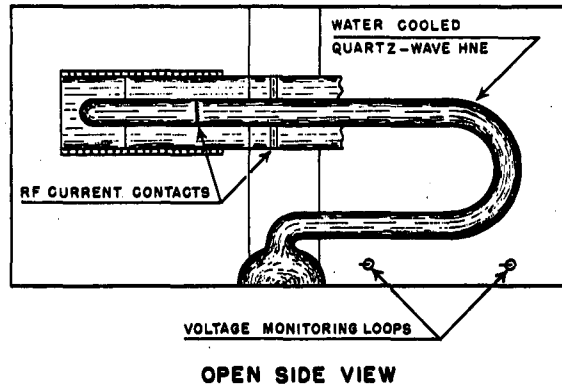
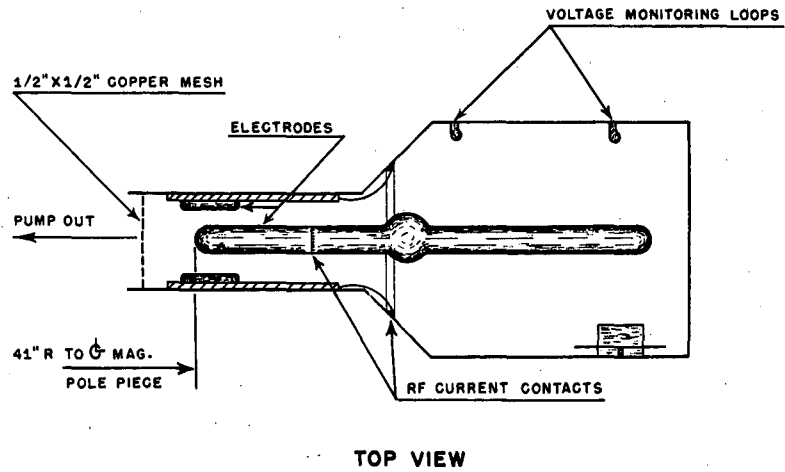


Fig. 1 - Drawing of Test Cavity

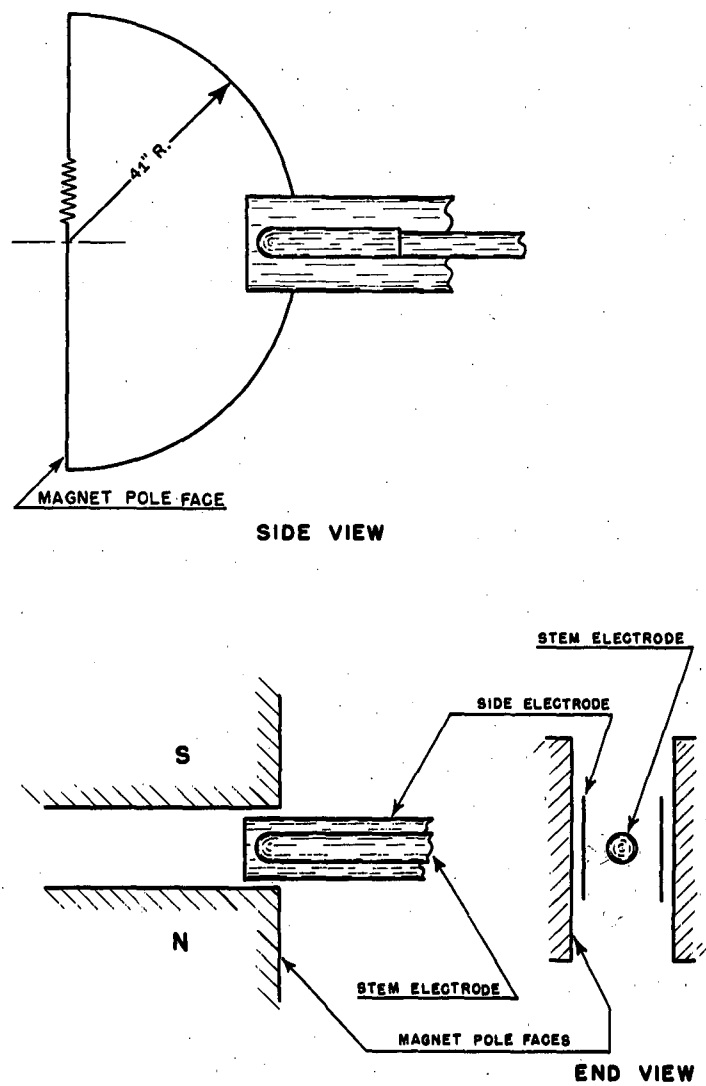
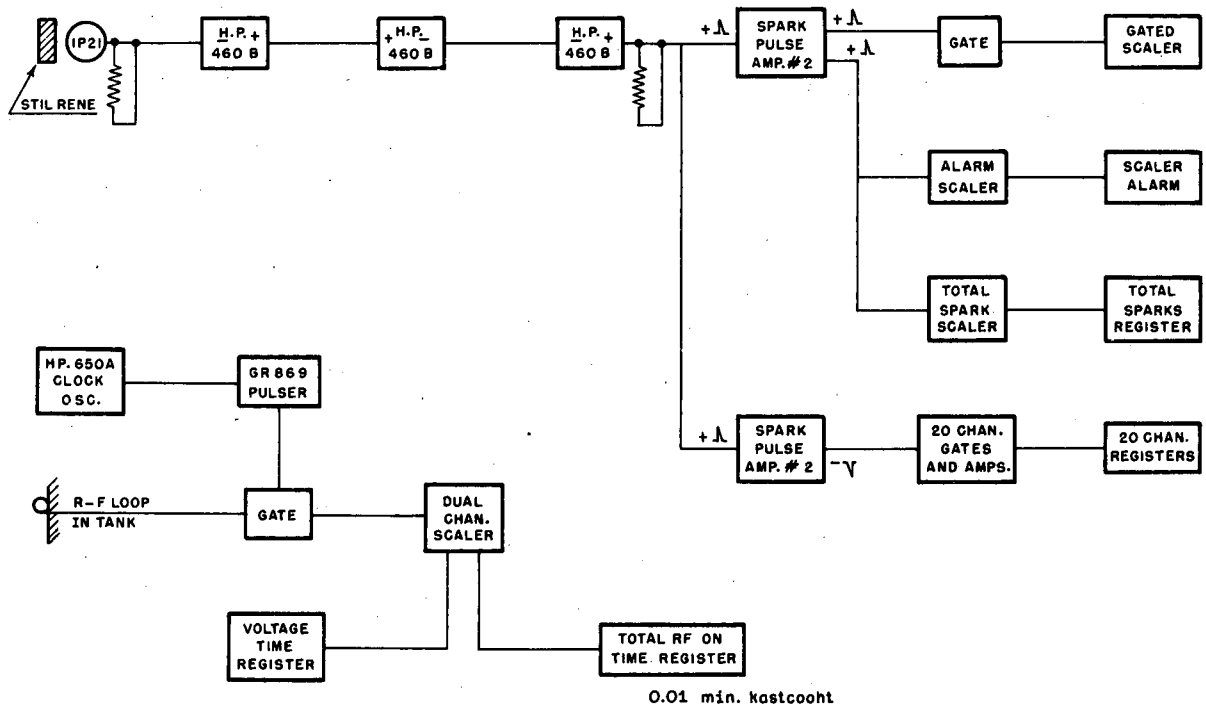


Fig. 2 - Test Geometry



MU-4347

Fig. 3 - Spark Monitoring Circuits

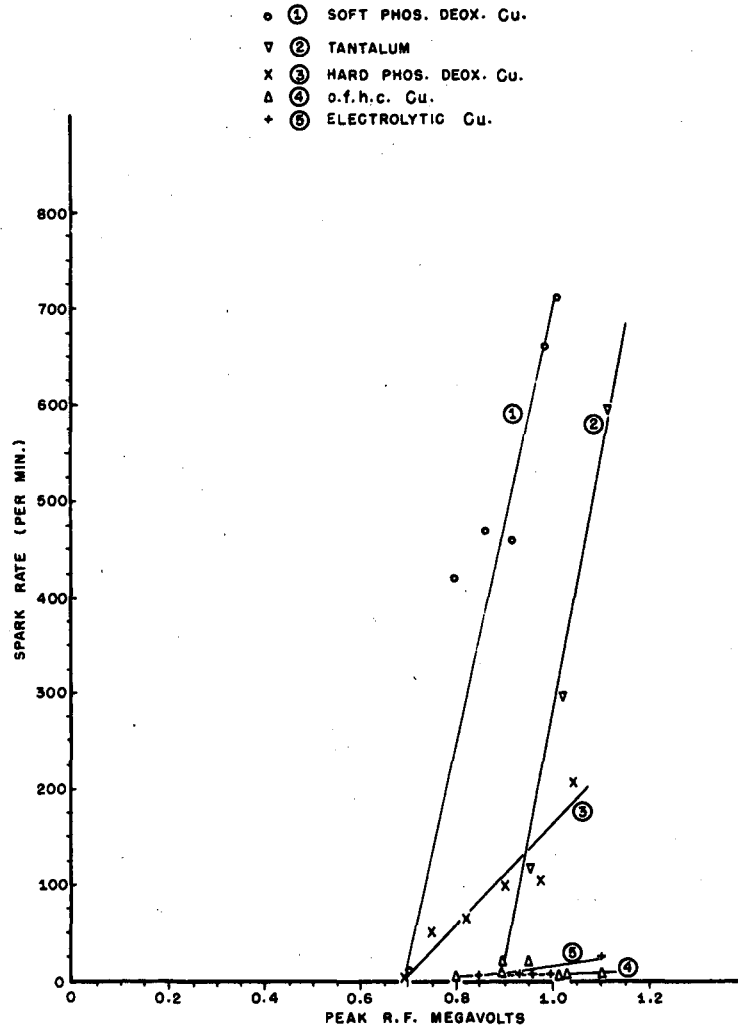


FIGURE 4

MU-4348

Fig. 4 - Sparking Rate Versus Voltage Curves

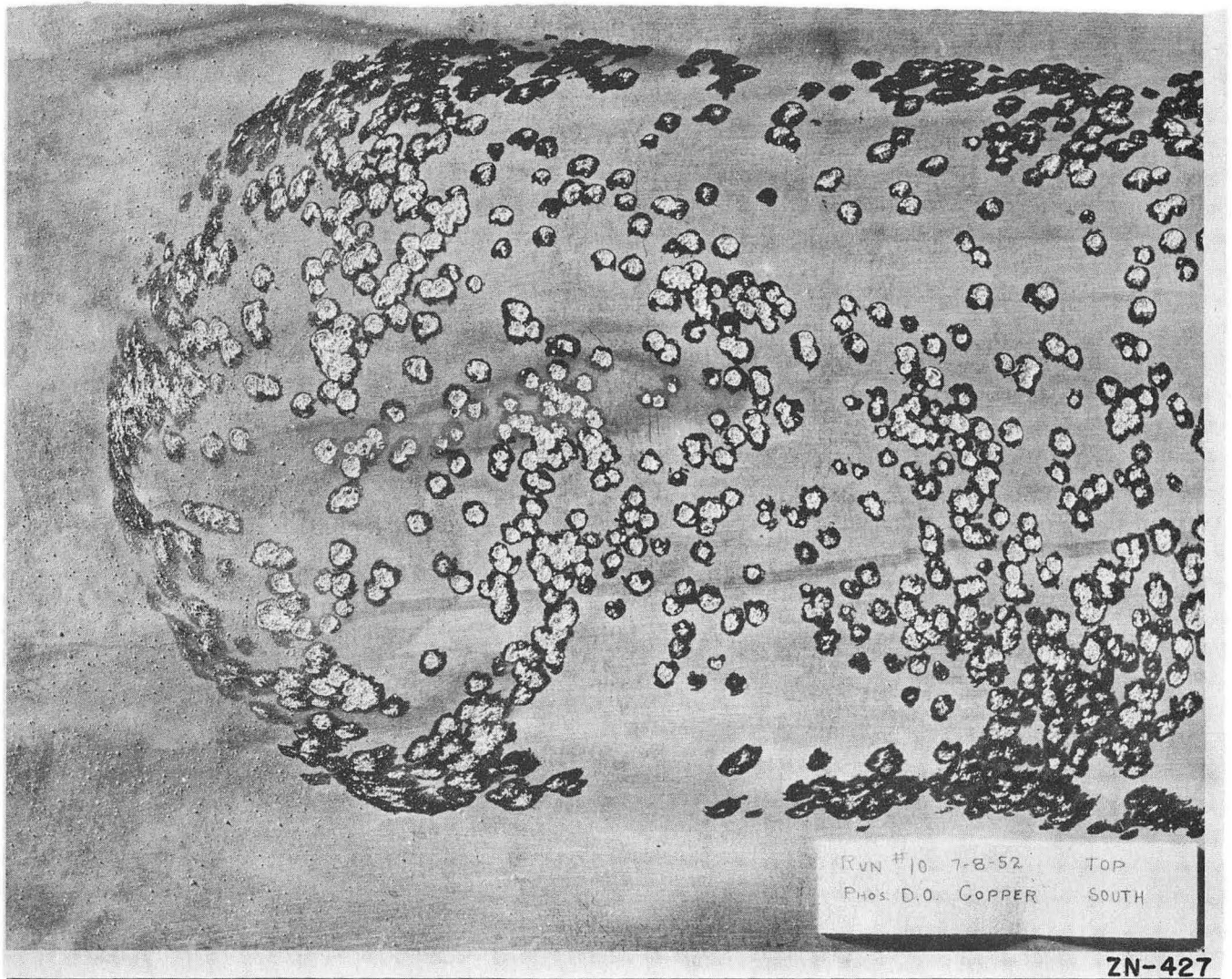


Fig. 5 - DHP Copper Side Electrode

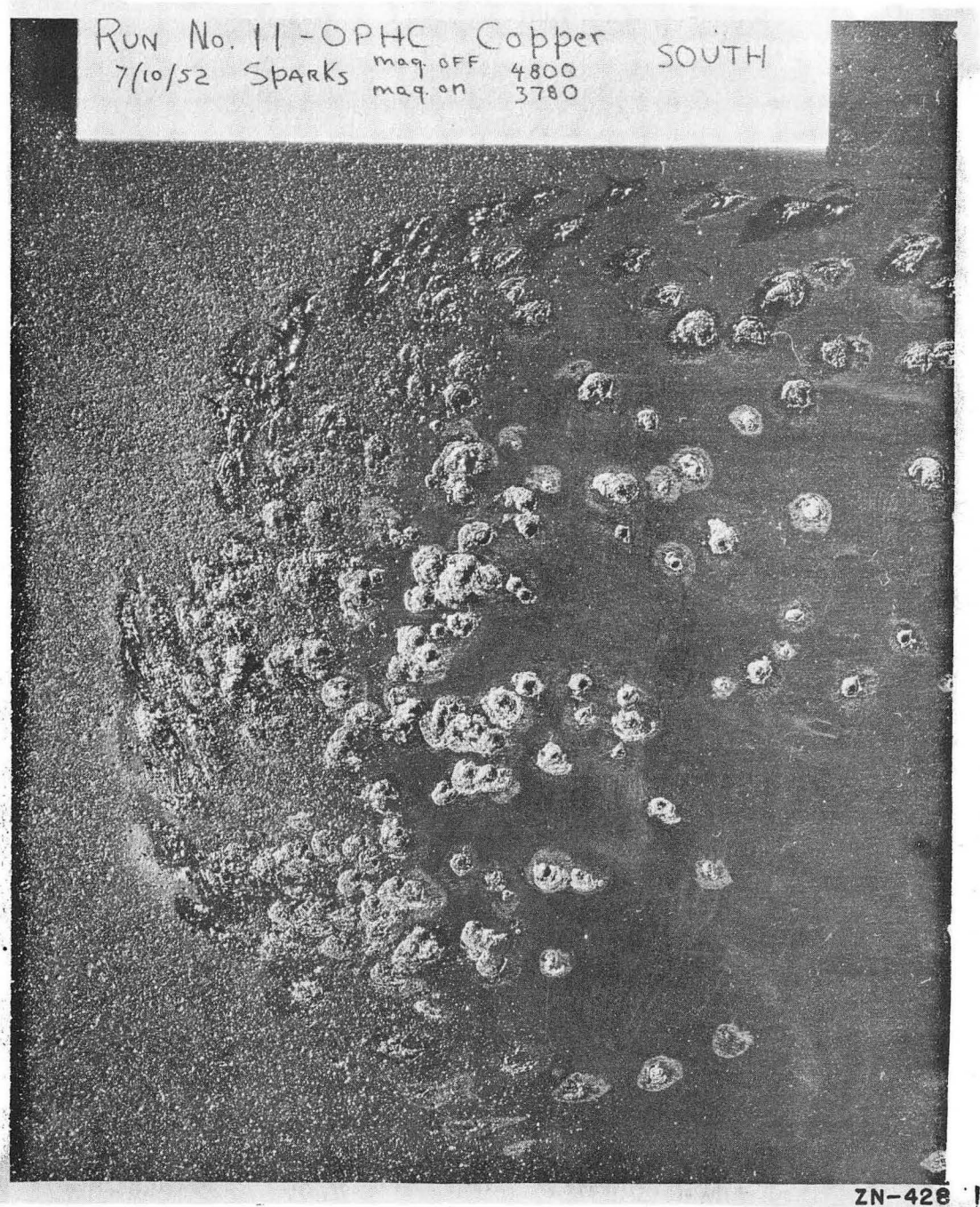


Fig. 6 - OFHC Copper Side Electrode

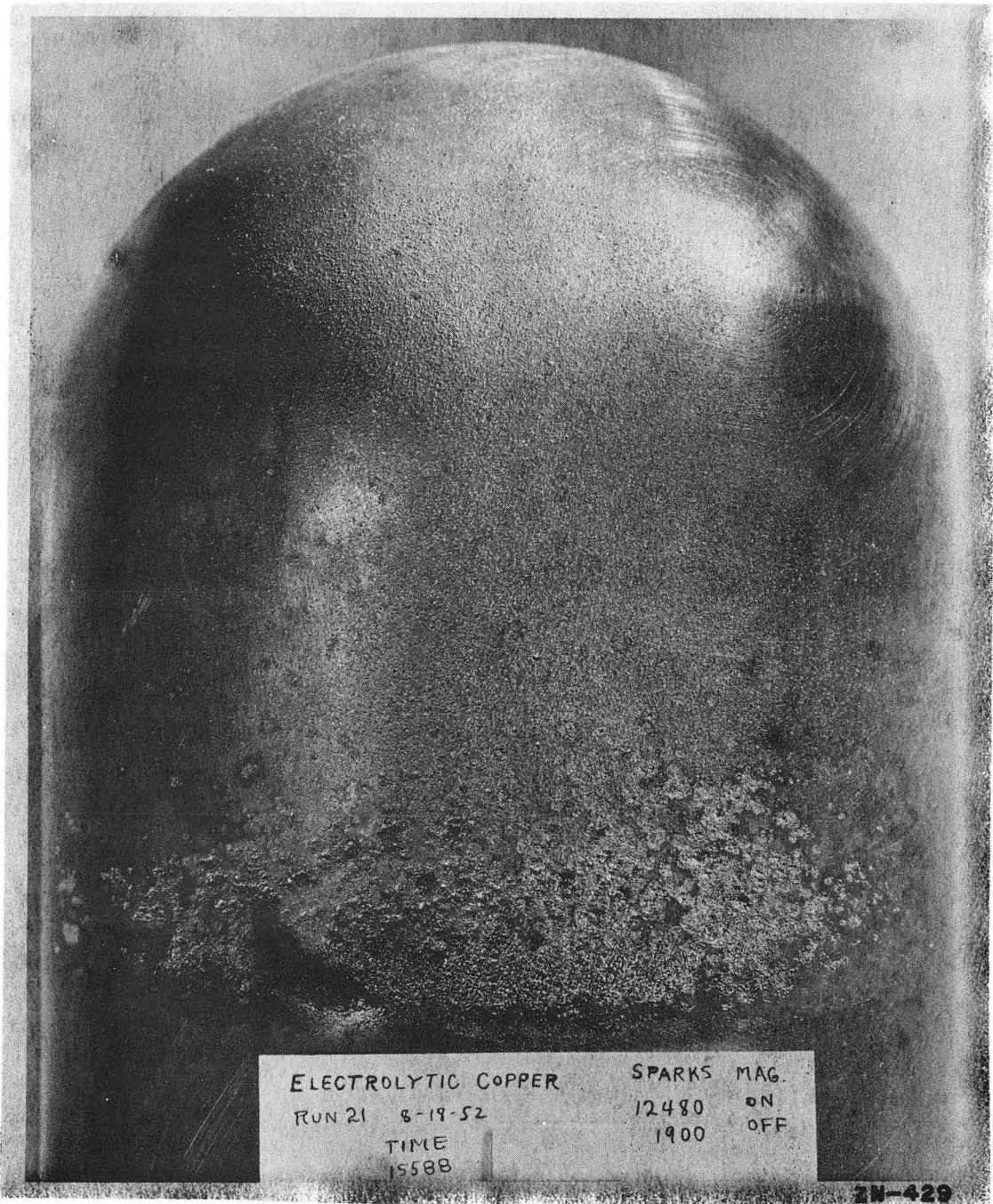


Fig. 7 - ETP Copper Stem Electrode



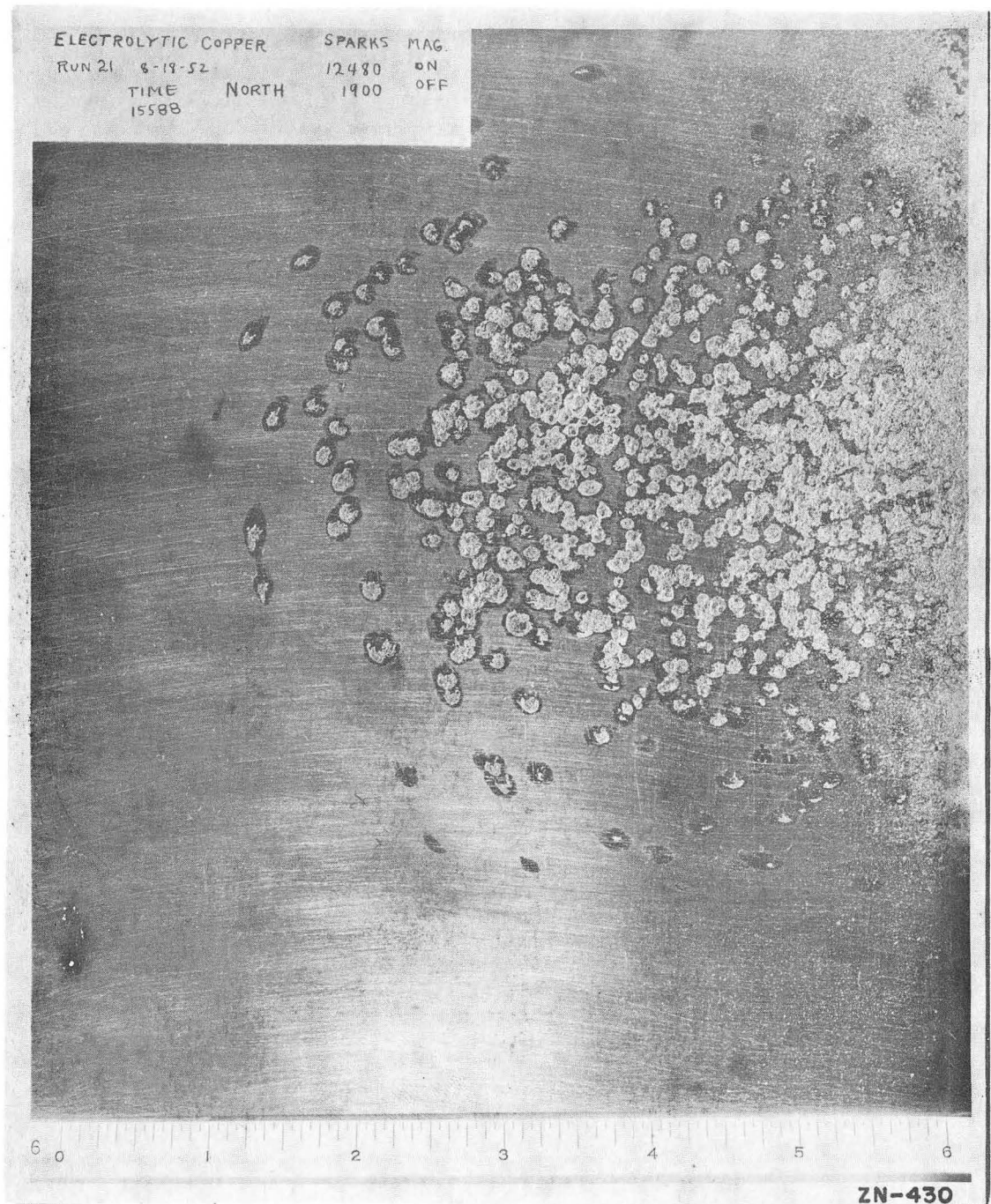


Fig. 8 - ETP Copper Side Electrode



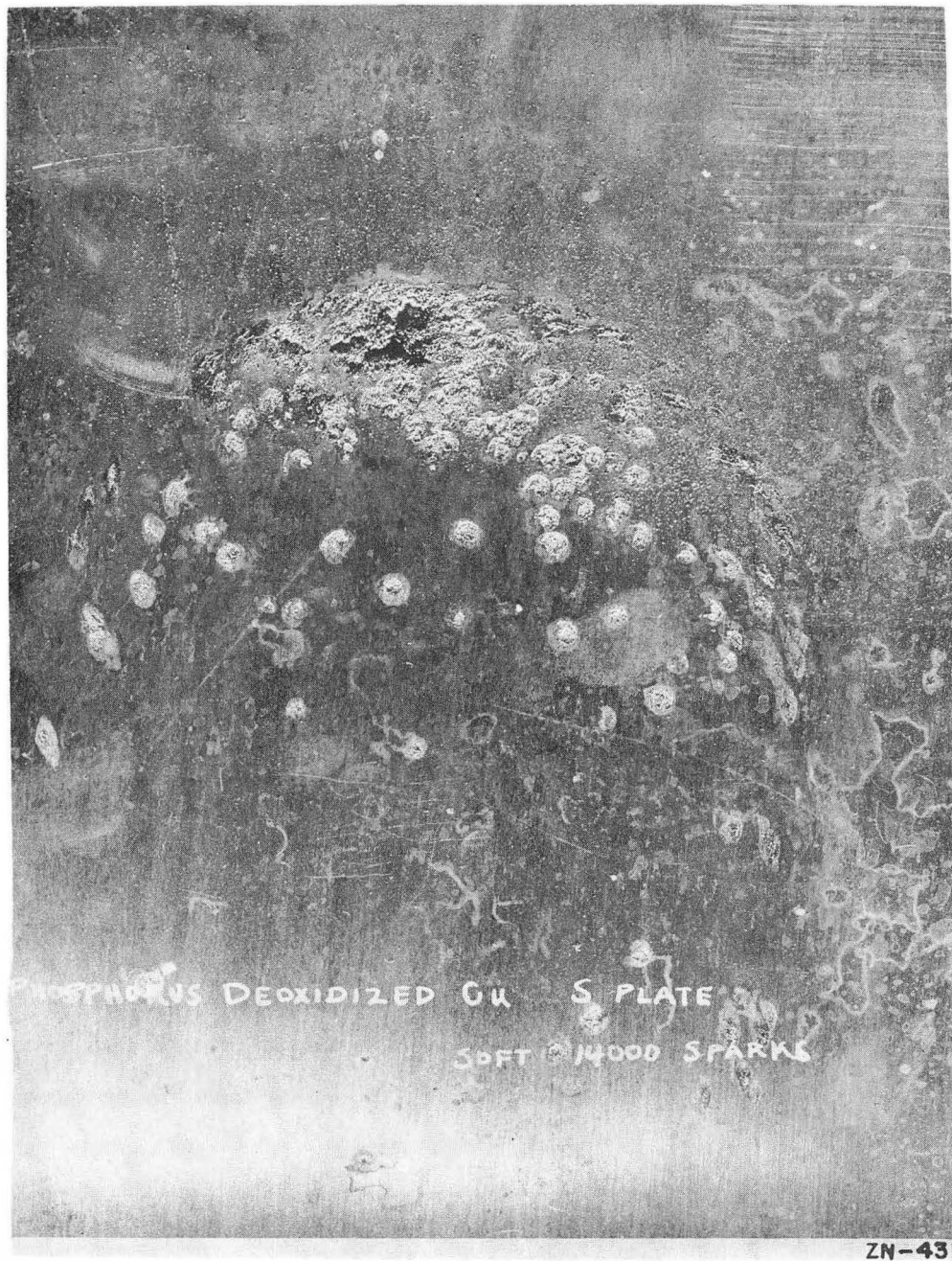
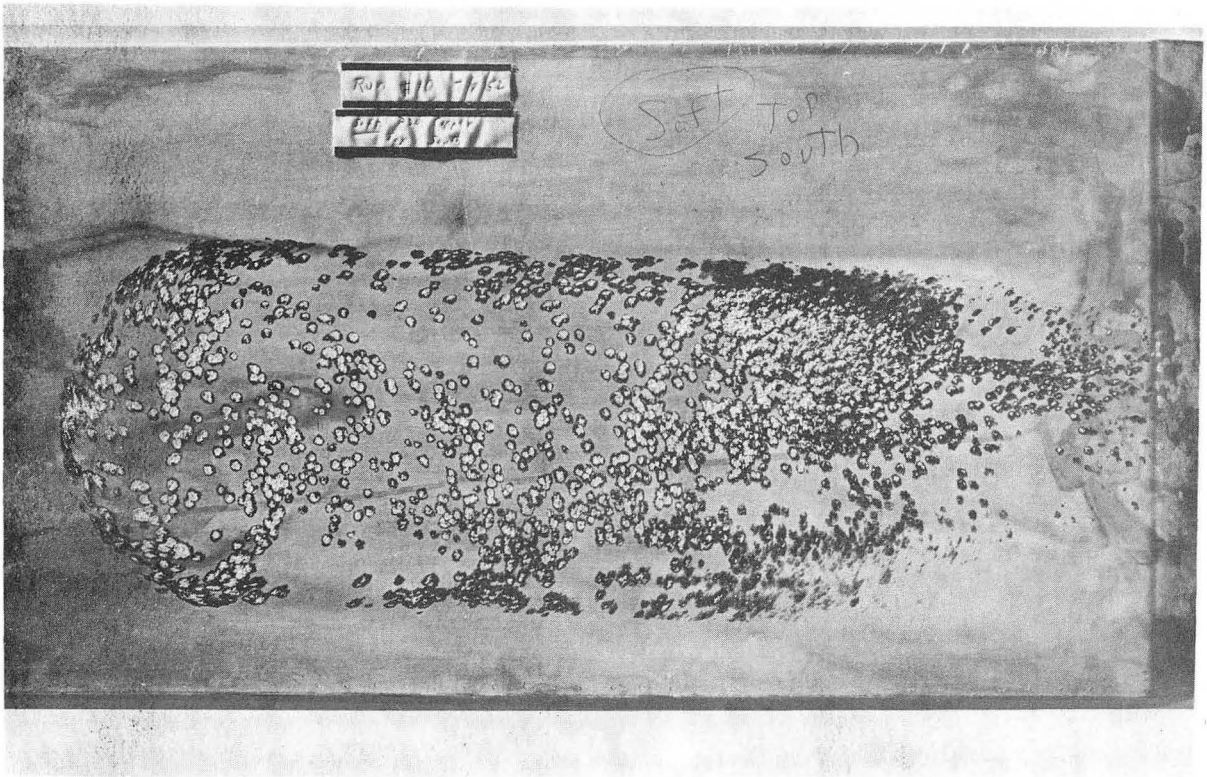


Fig. 9 - Eroded DHP Copper  
Side Electrode



Fig. 10 - Shot-Blasted DHP Copper  
Side Electrode



ZN-433

Fig. 11 - Fully Annealed DHP  
Copper Side Electrode



Fig. 12 - Tantalum Stem Electrode



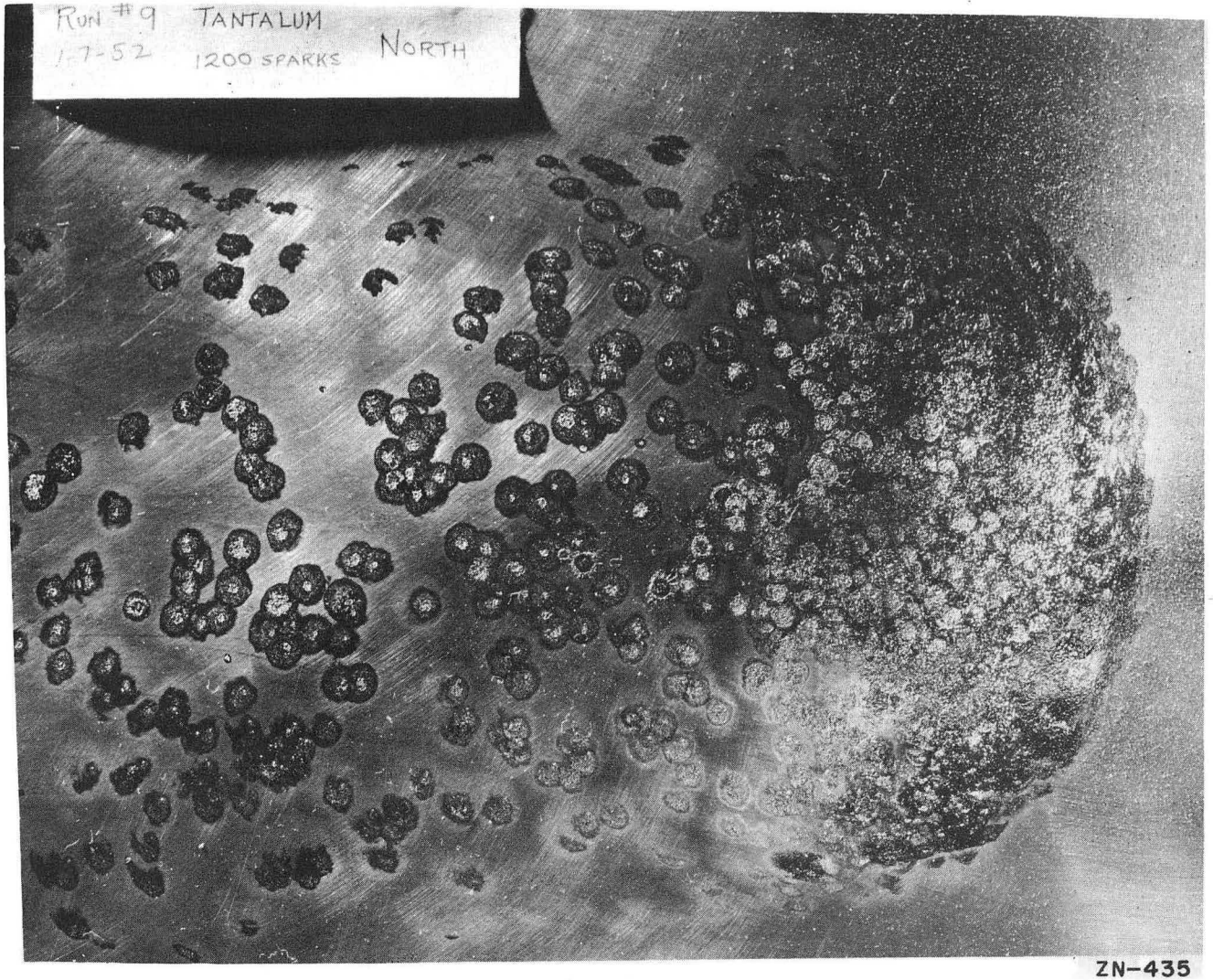


Fig. 13 - Tantalum Side Electrode



ZN-436

Fig. 14 - Molybdenum Stem Electrode



Fig. 15 - Molybdenum Side Electrode



Fig. 16 - Inconel Side Electrodes





Fig. 17 - Inconel Side Electrodes

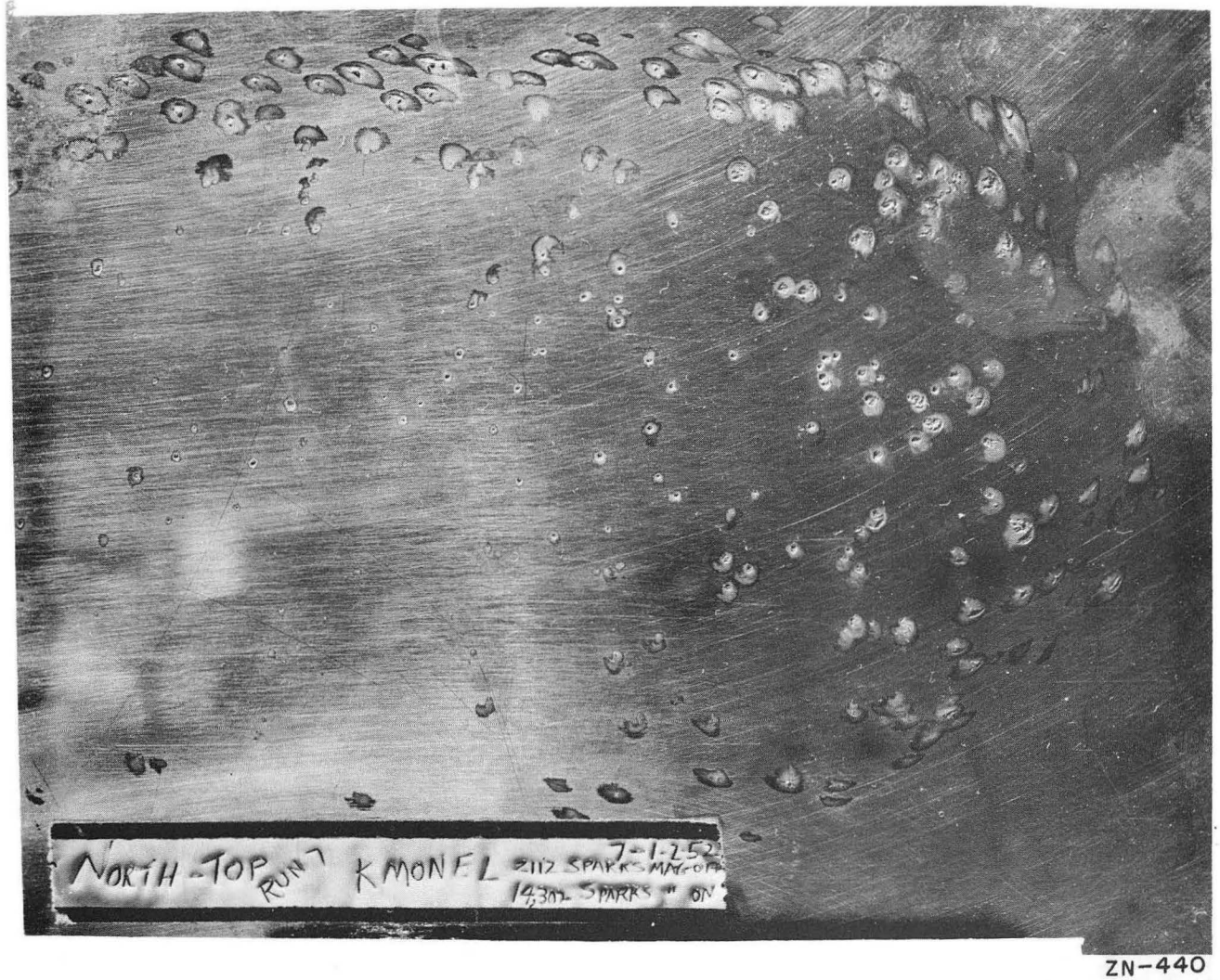


Fig. 18 - K-Monel Side Electrode



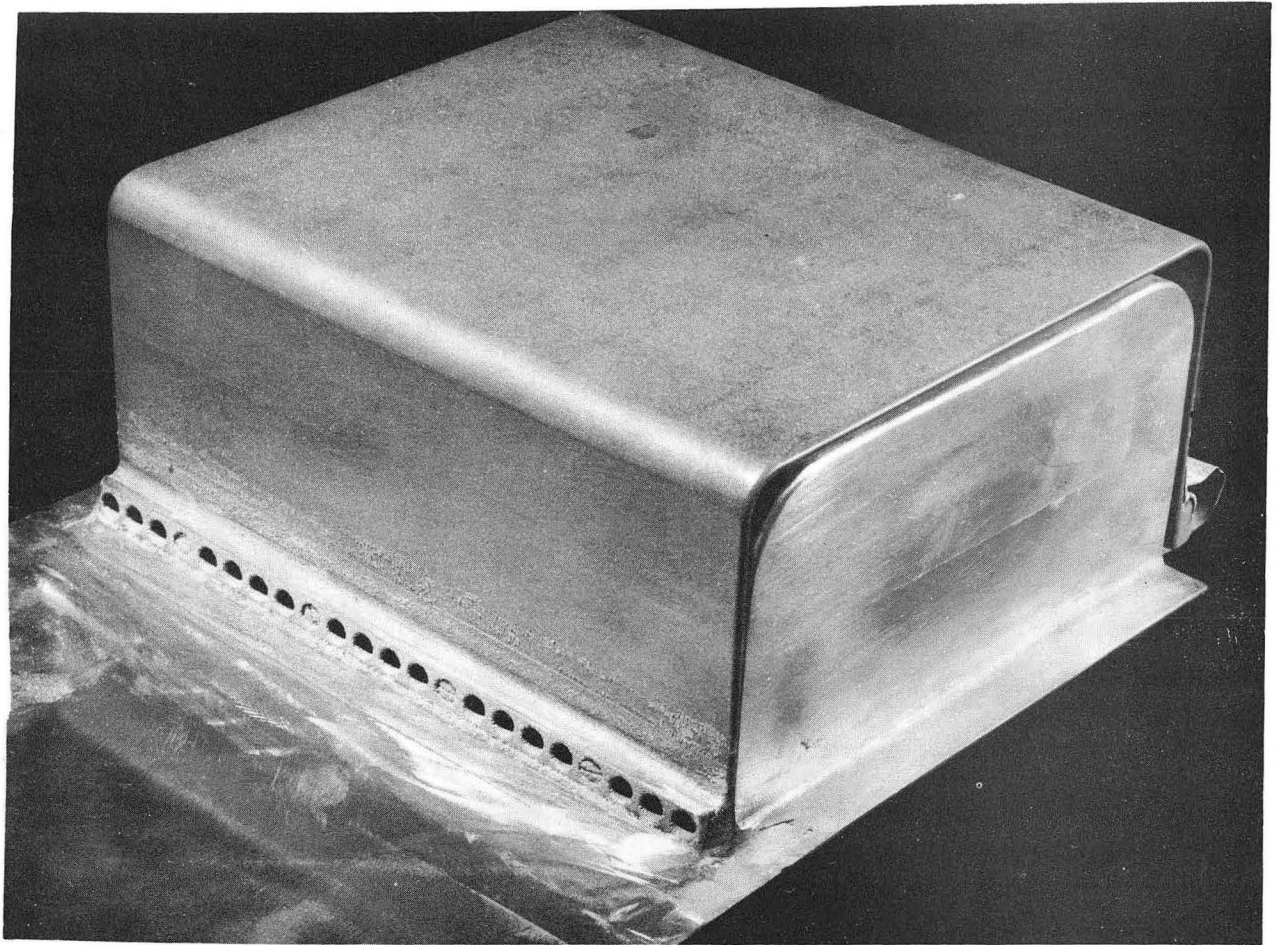
Fig. 19 - C-18 Carbon Stem Electrode  
Showing Details of RF Contacts



ZN-442

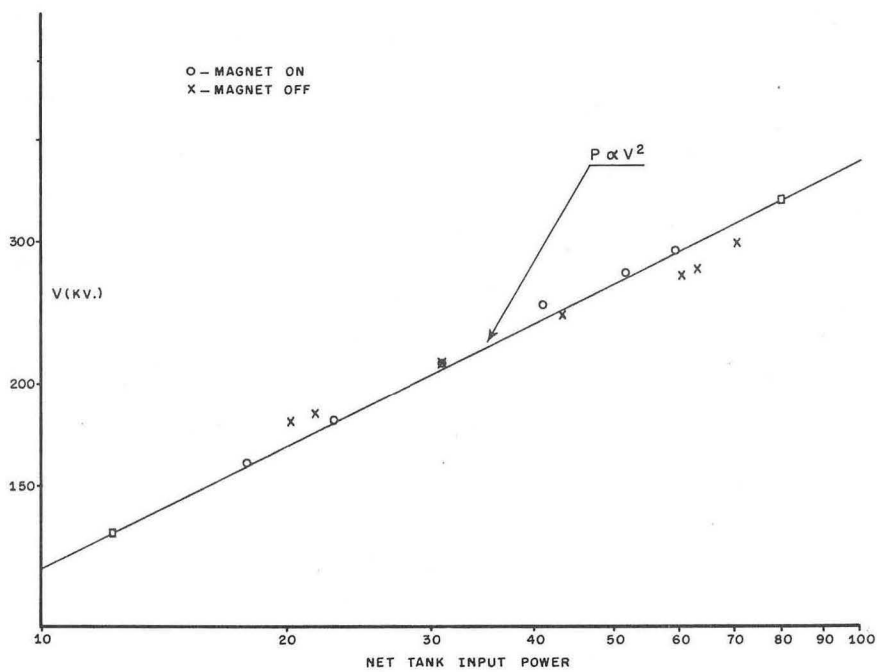
Fig. 20 - C-18 Carbon Side Electrodes  
Showing Details of RF Contacts and  
Thermal Expansion Joints





ZN-443

Fig. 21 - C-18 Carbon Side Electrodes  
Showing Details of RF Contacts and  
Thermal Expansion Joints



MU-4349

Fig. 22 - Peak RF Voltage Versus Power Input for C-18 Carbon Electrodes

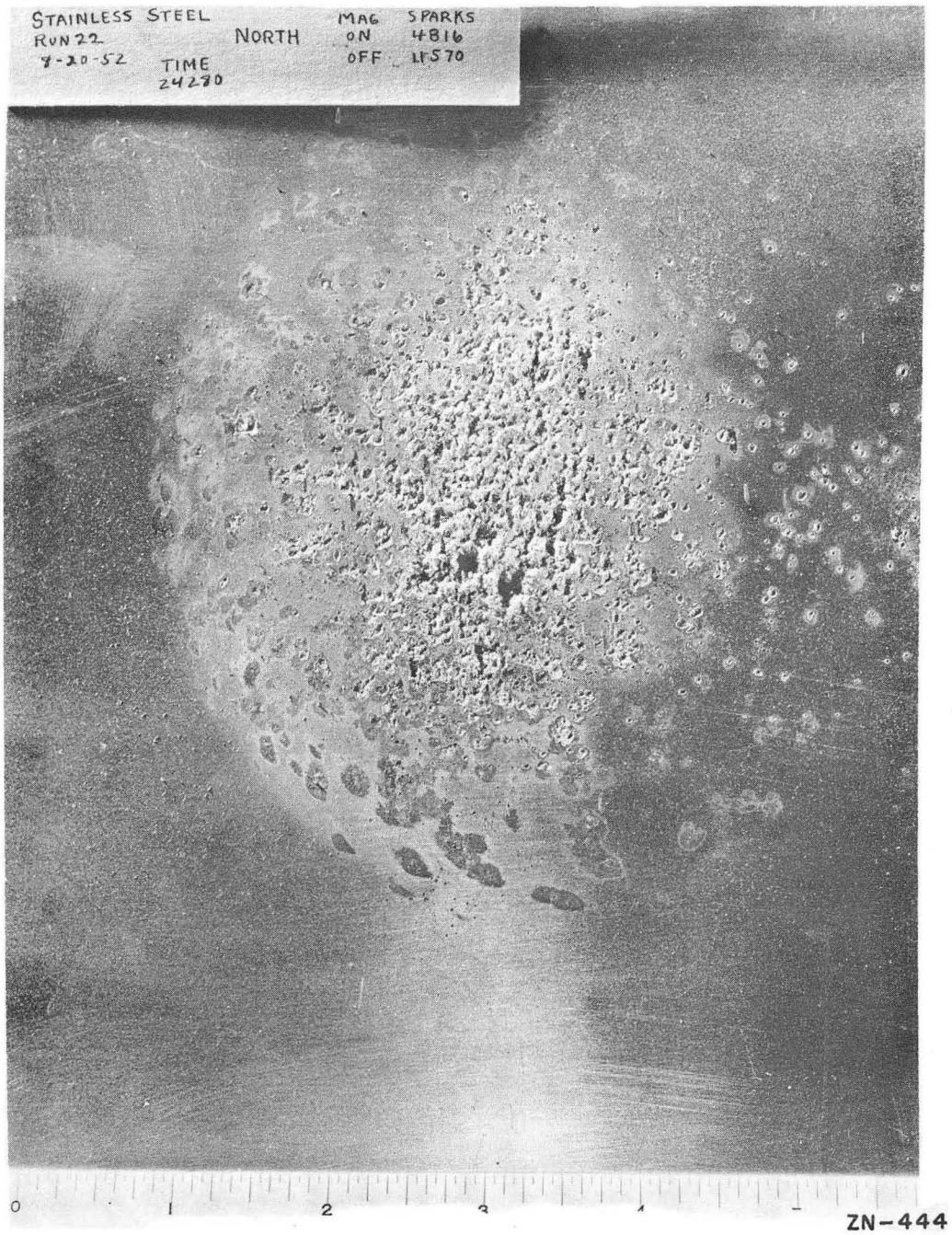


Fig. 23 - Type 316 Stainless Steel  
Side Electrodes

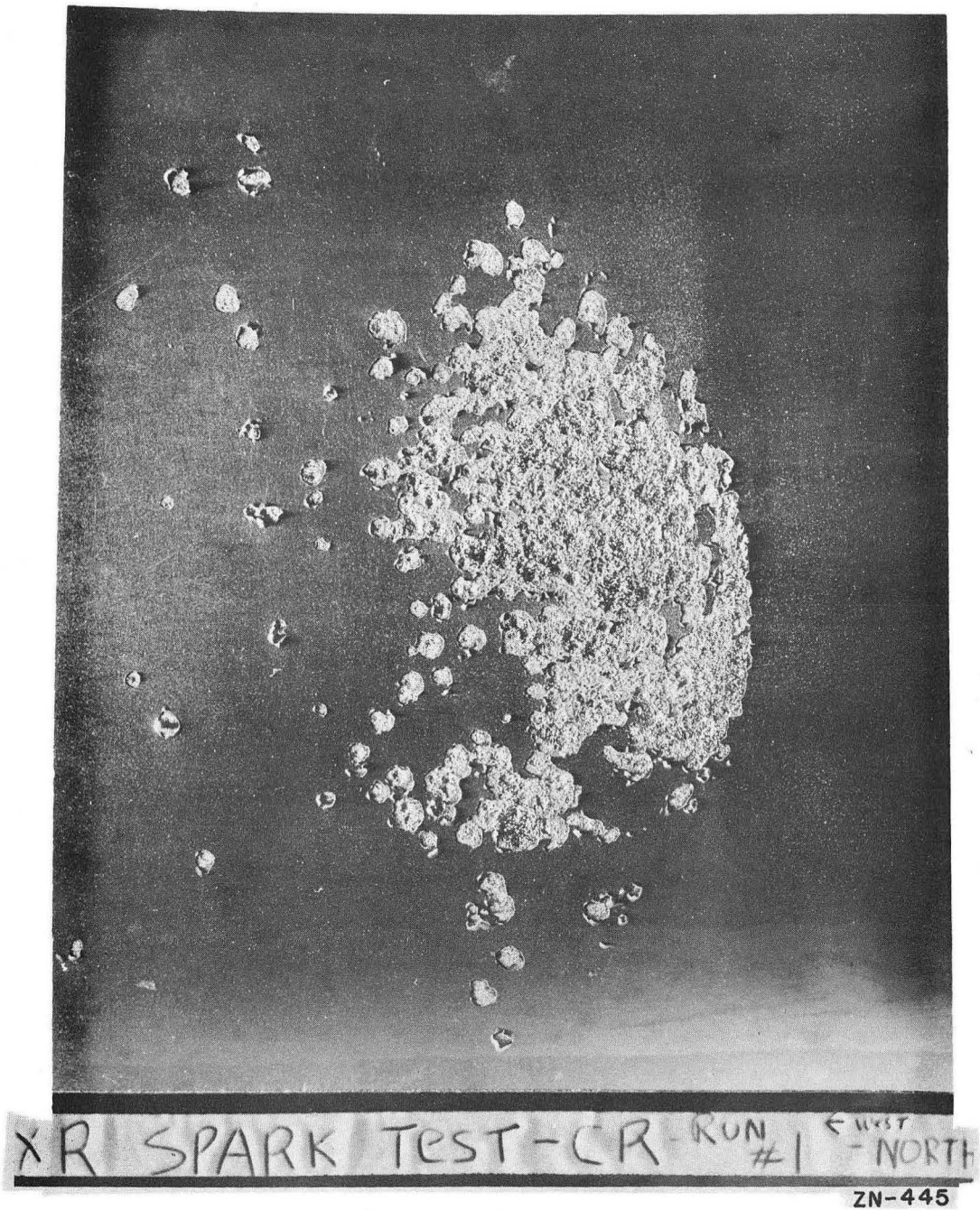


Fig. 24 - Satin Chrome-Plated Copper  
Side Electrode



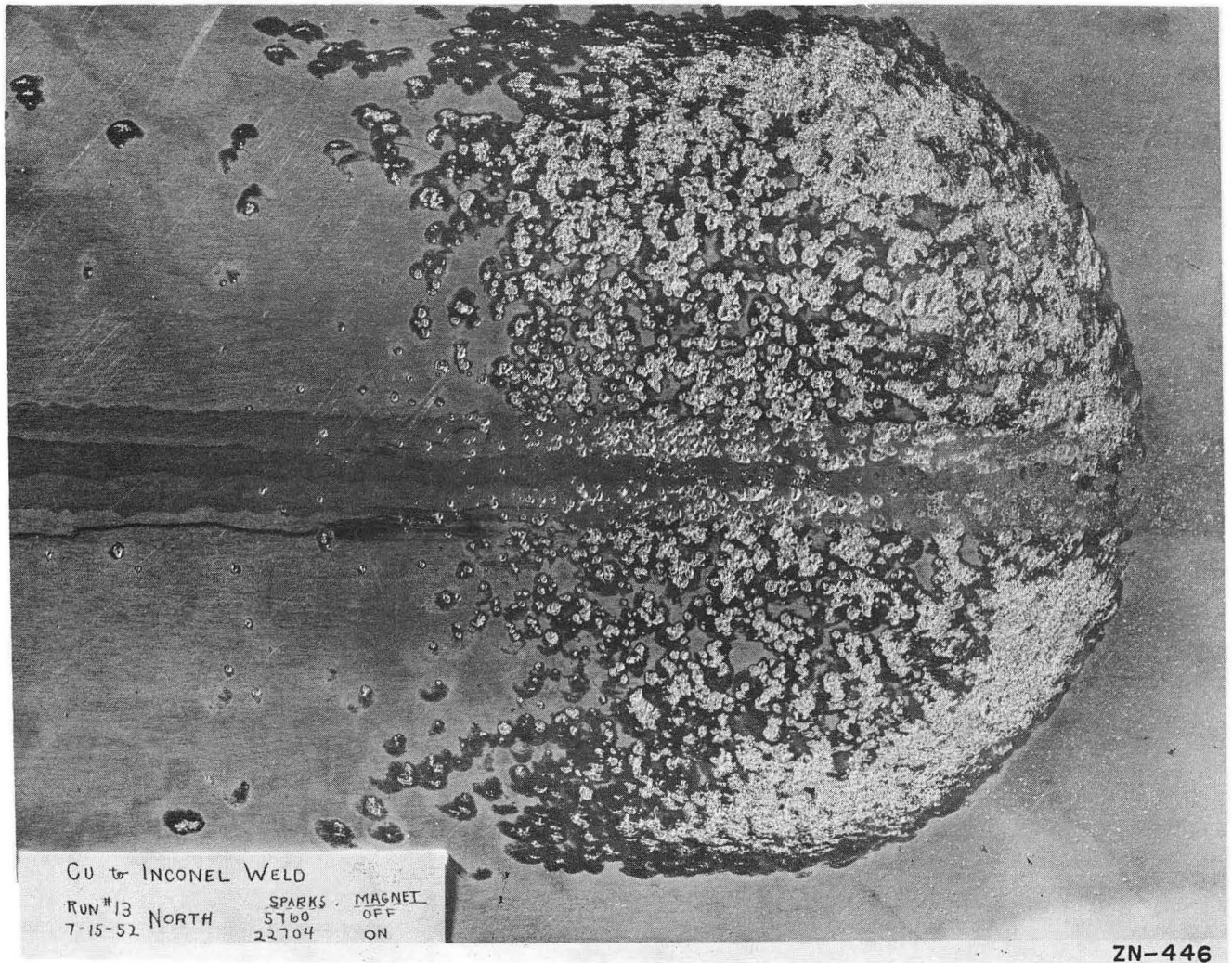


Fig. 25 - Inconel To DHP Copper Weld

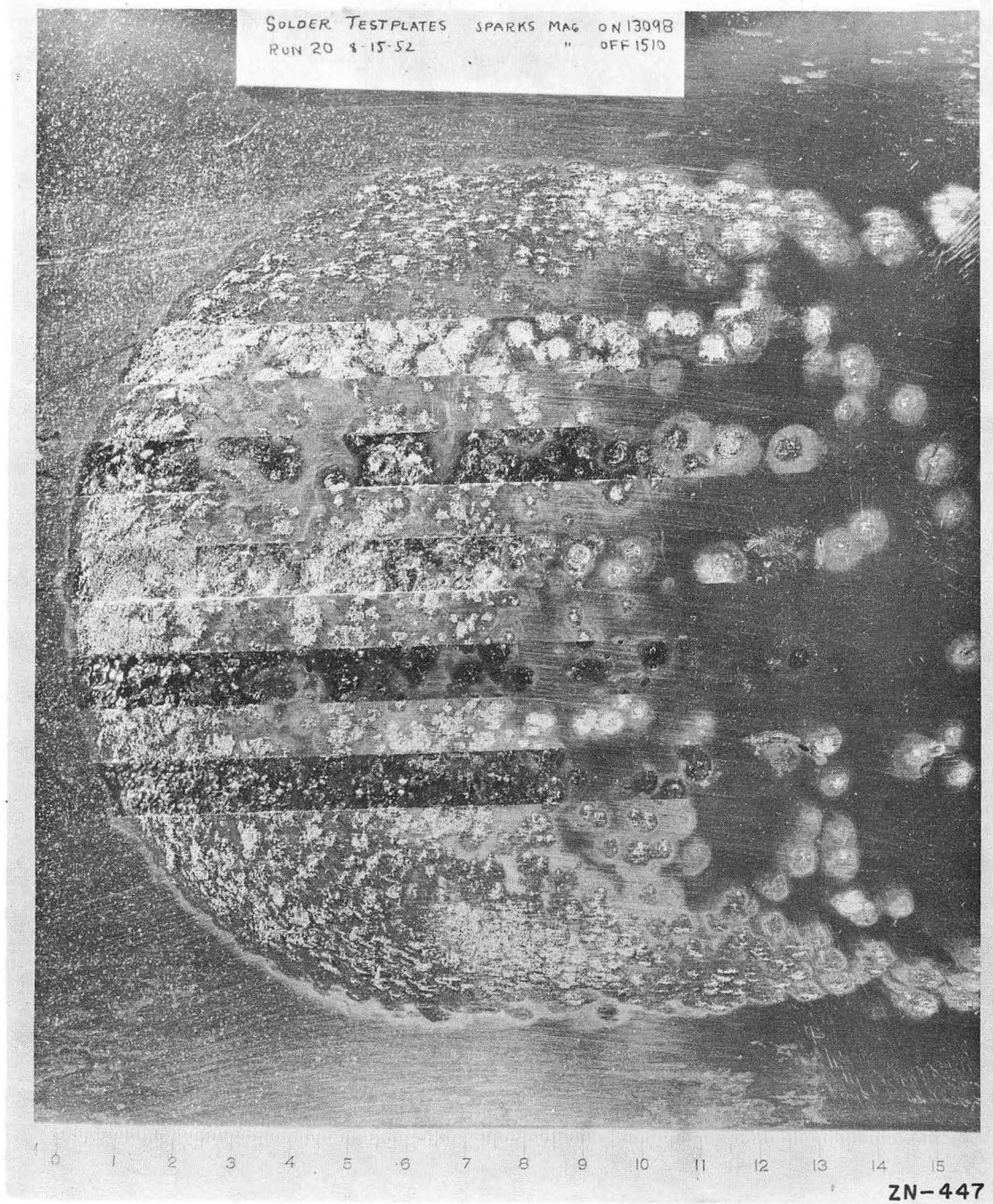
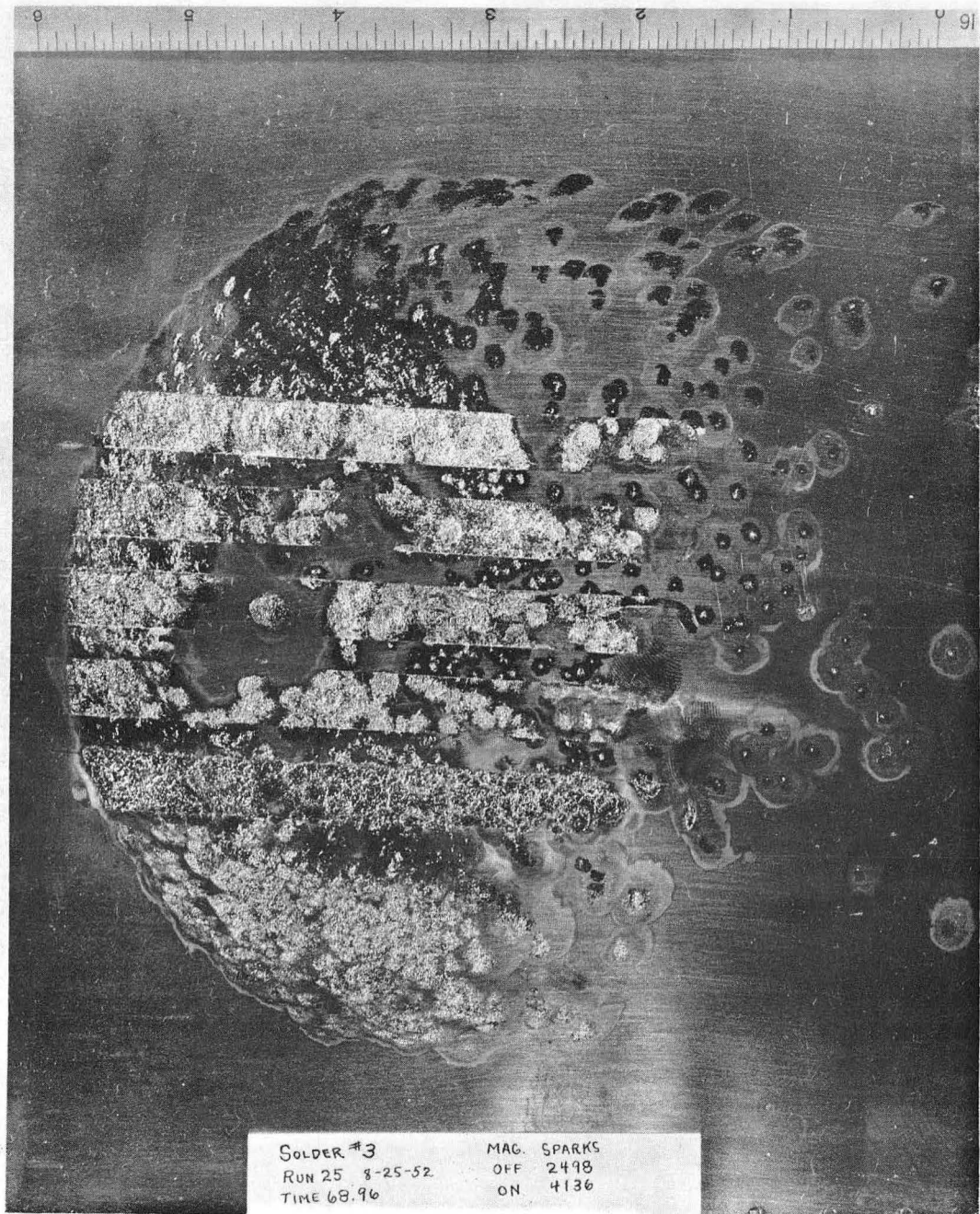


Fig. 26 - Solder Test No. 1



ZN-448

Fig. 27 - Solder Test No. 2



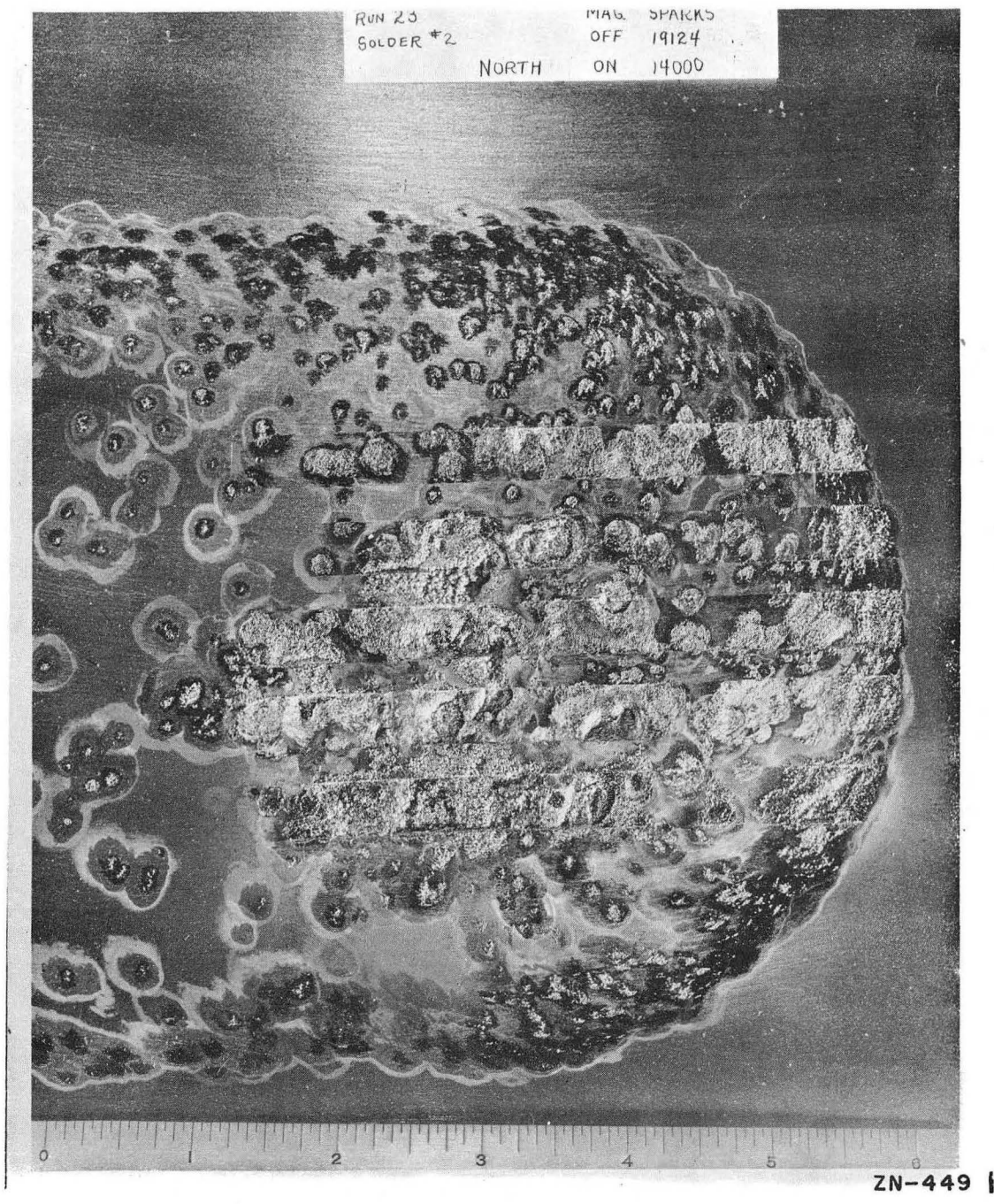


Fig. 28 - Solder Test No. 3

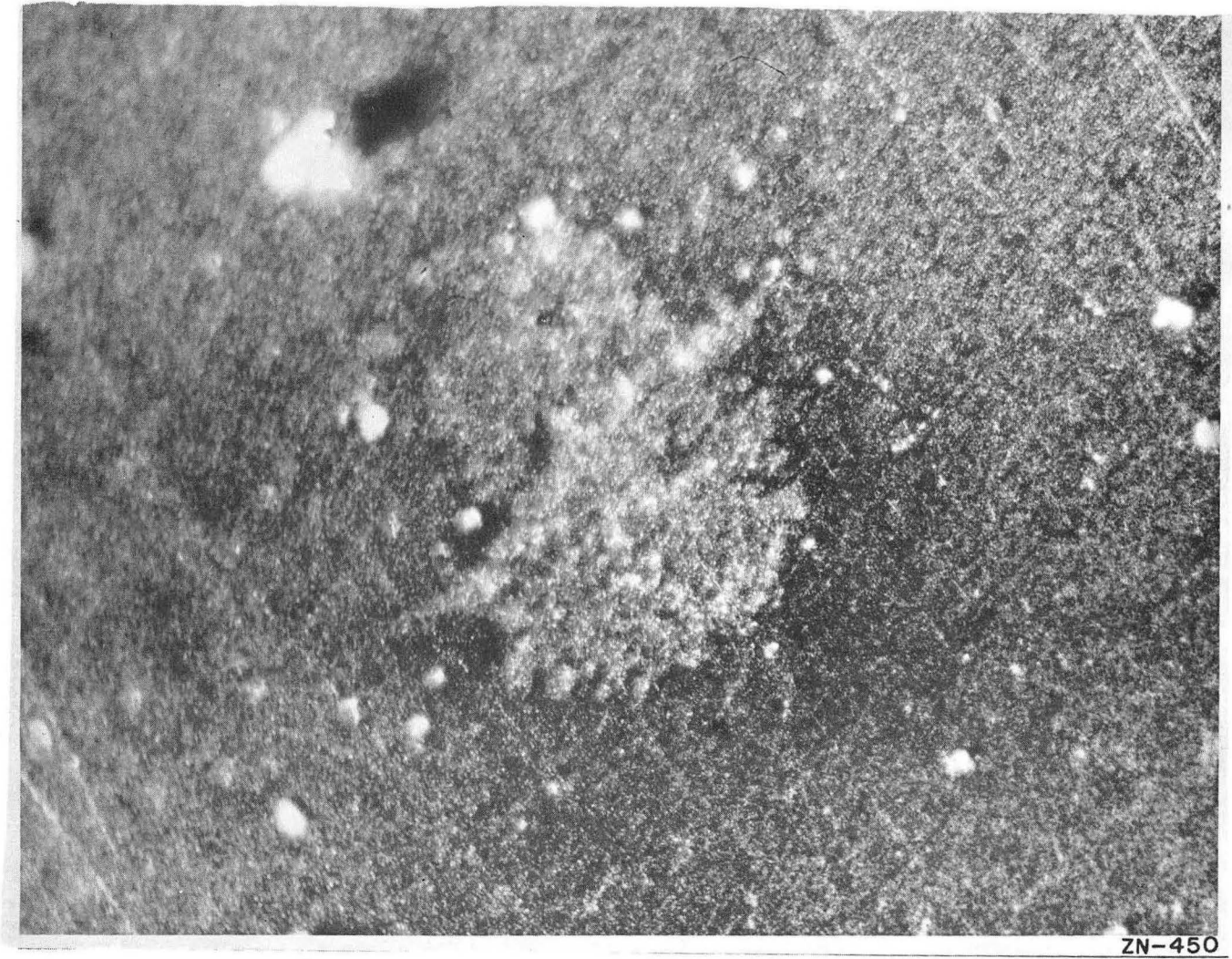


Fig. 29 - Photomicrographs of Spark  
Marks on Center Electrode



ZN-451

Fig. 30 - Photomicrographs of Spark  
Marks on Center Electrode



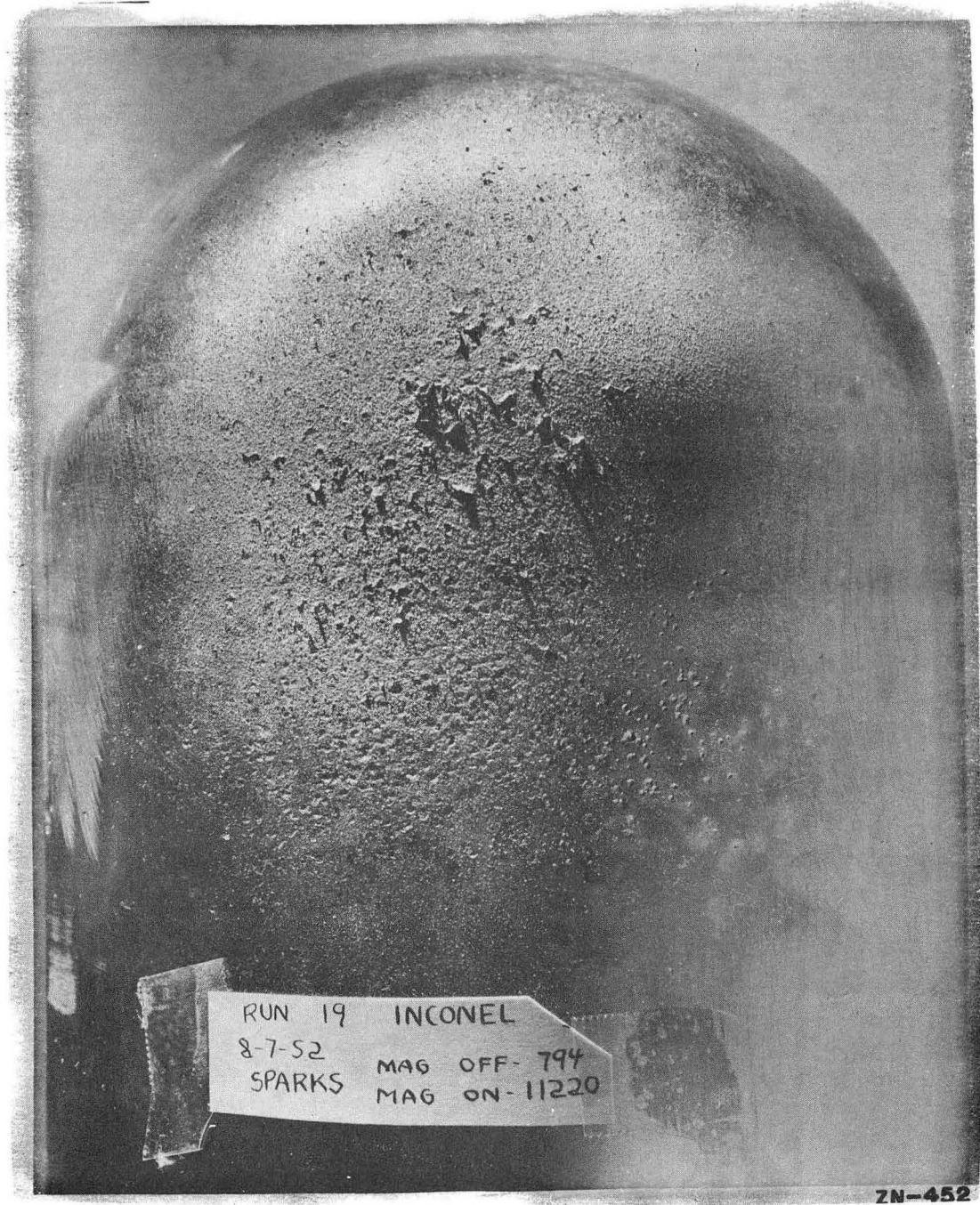
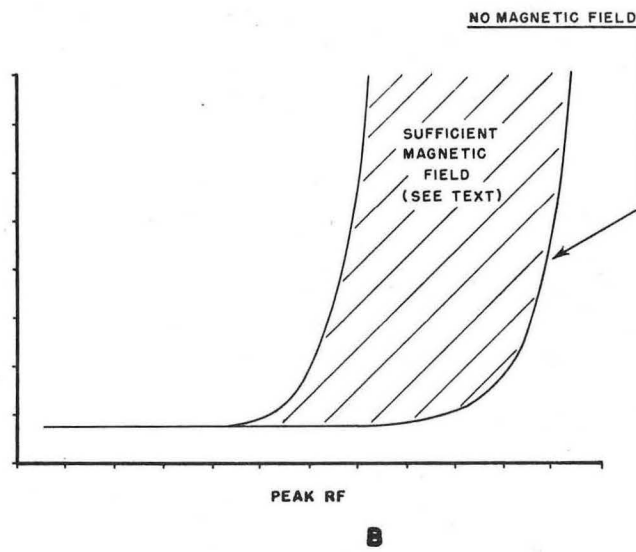
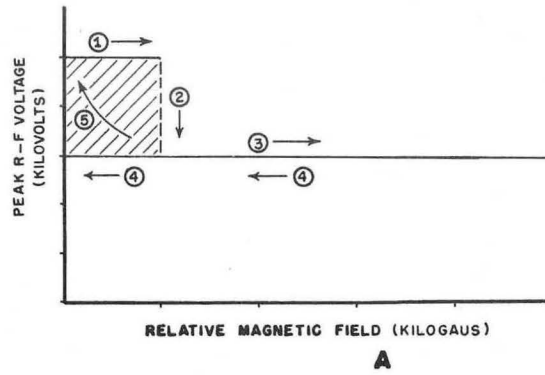


Fig. 31 - Cracking and Peeling of Thick Sputtered Material on Stem Electrode



MU-4350

Fig. 32 - (a) Variation of Breakdown Voltage with Magnetic Field  
 (b) Variation of Sparking Rate with Magnetic Field



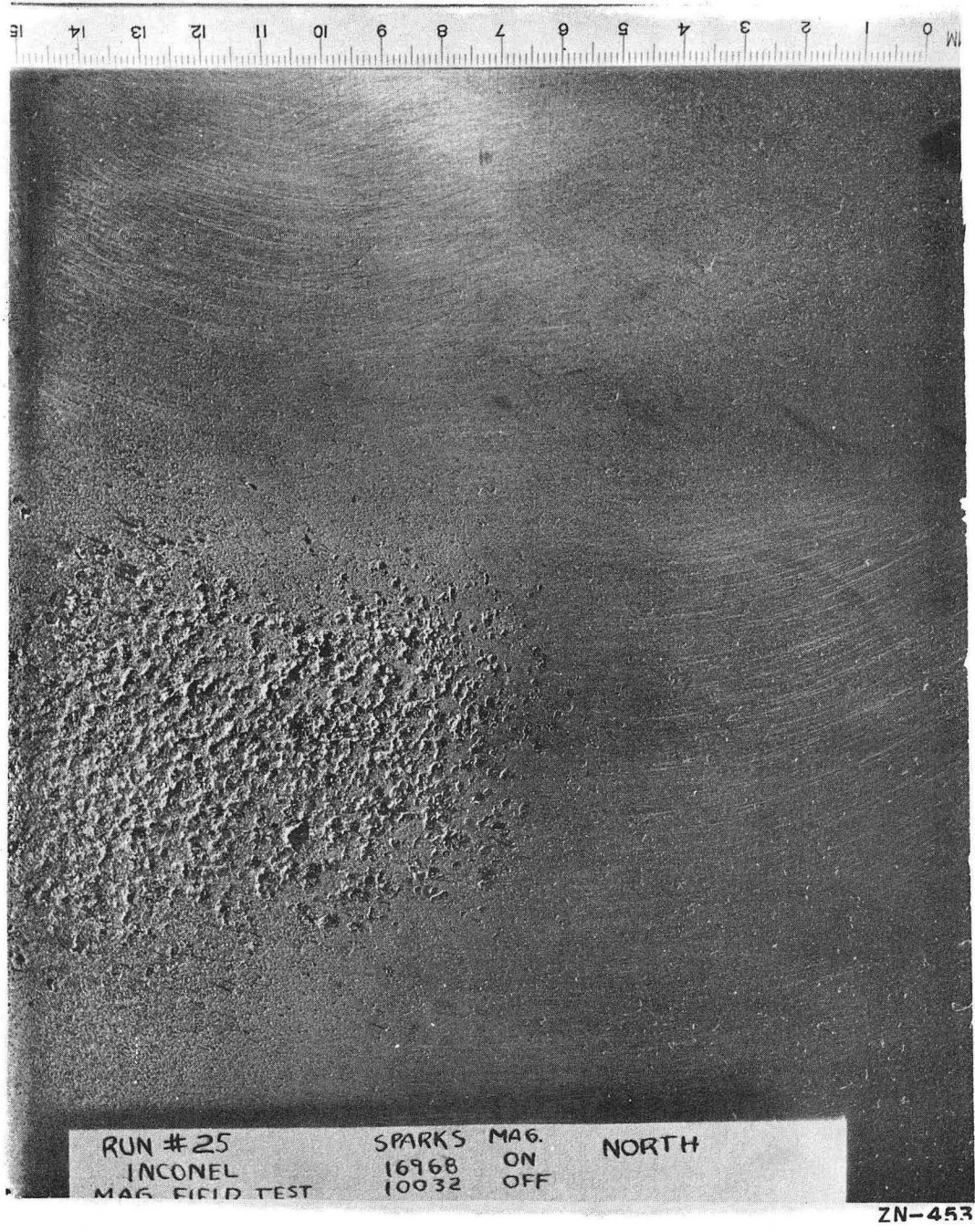


Fig. 33 - Spark Damage Concentration on Closest Side Electrode

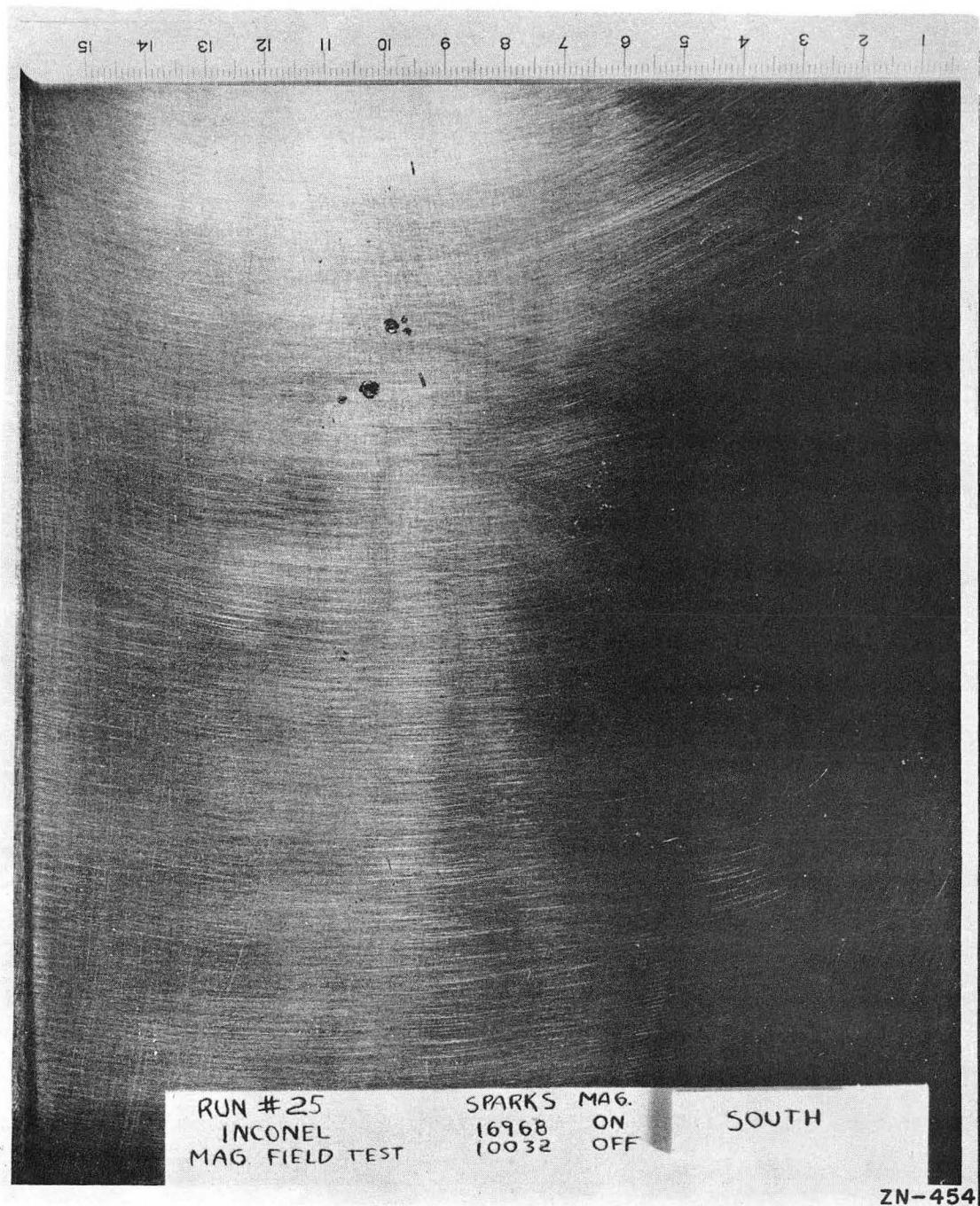
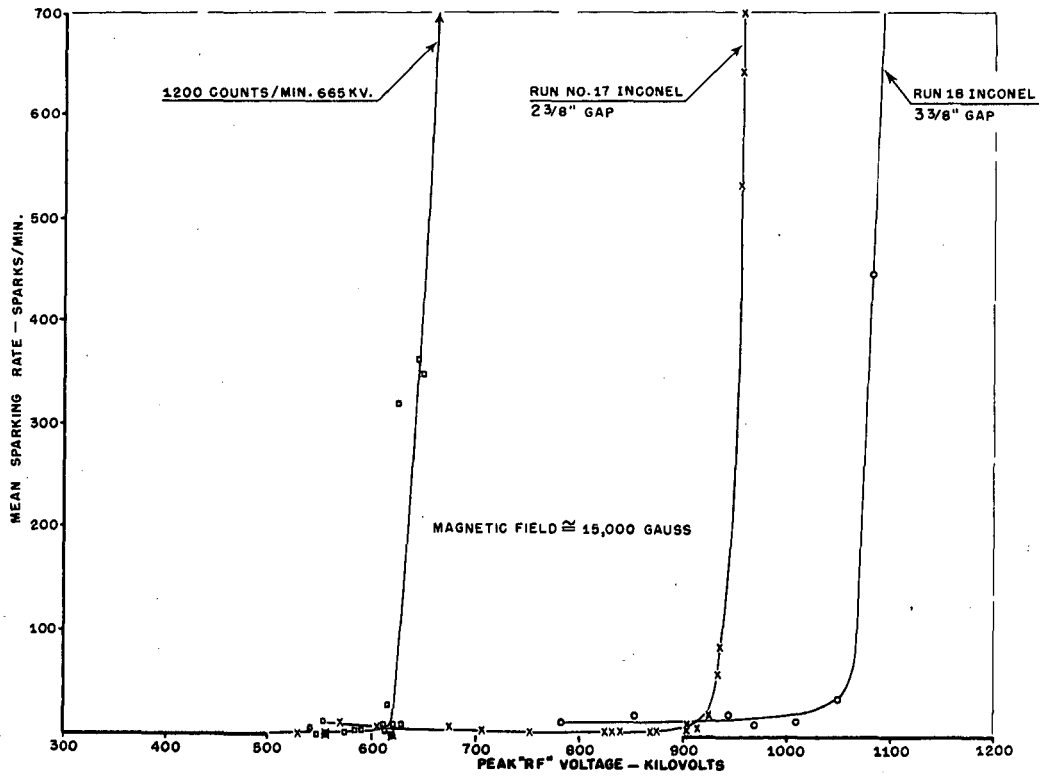
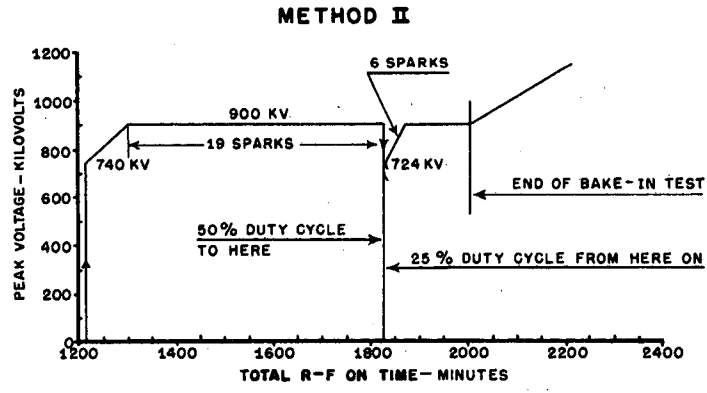
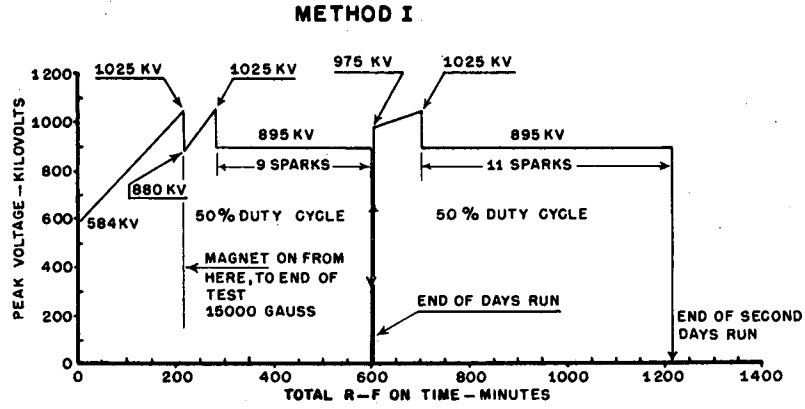


Fig. 34 - Spark Damage Concentration  
on Closest Side Electrode



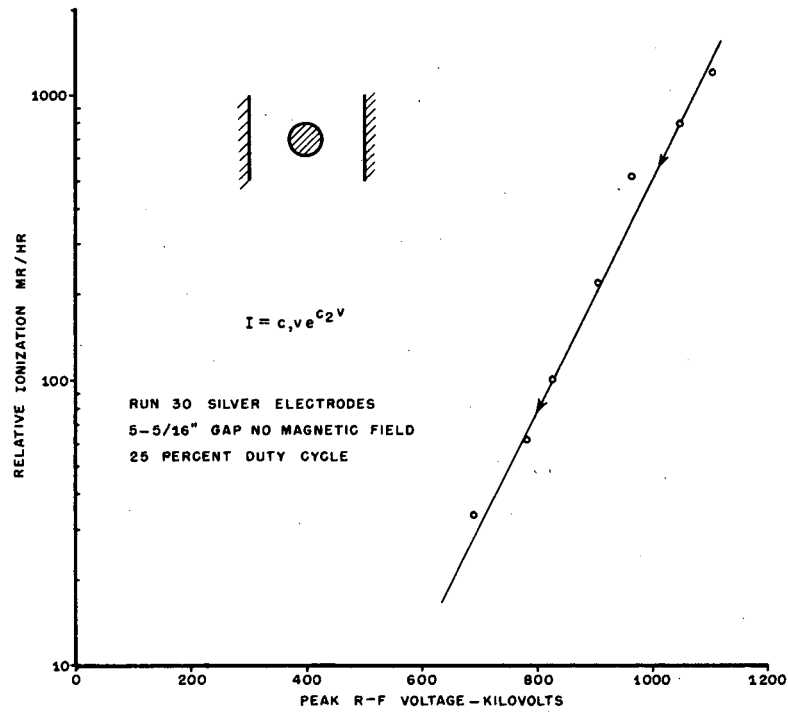
MU-4351

Fig. 35 - Sparking Rate Versus Voltage for Inconel



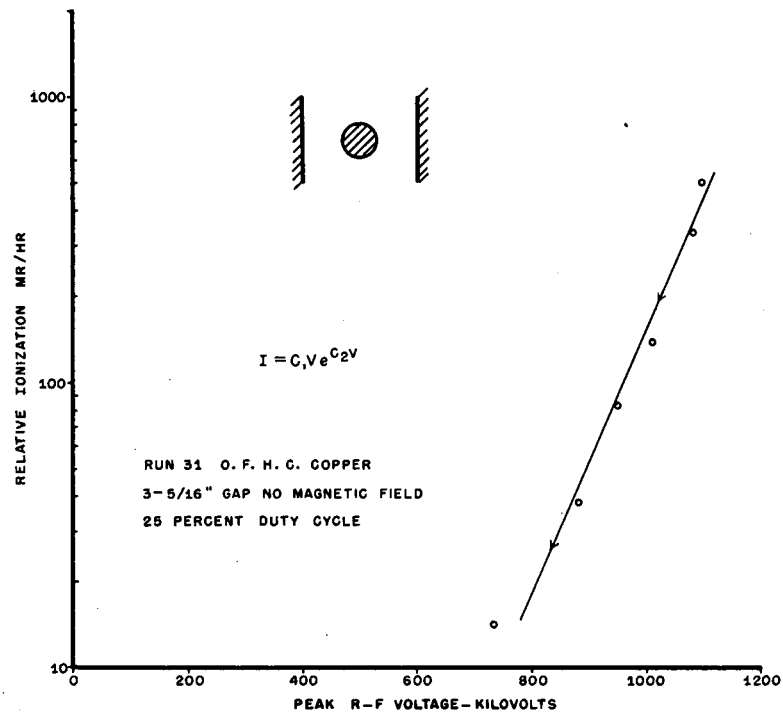
MU-4353

Fig. 36 - (a) and (b) Voltage Conditioning Schedule For Inconel



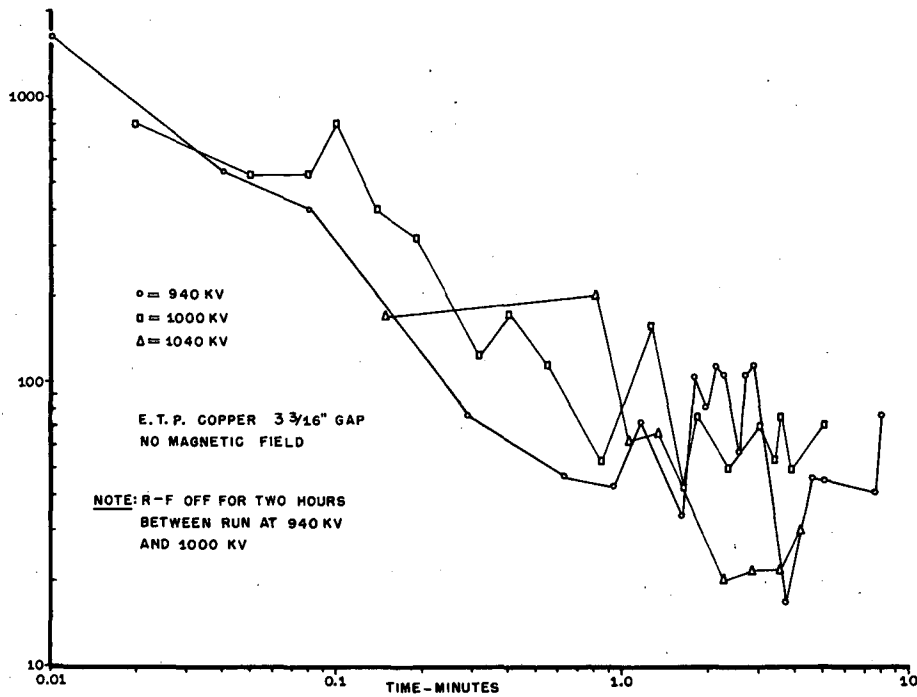
MU-4354

Fig. 37 - X-Ray Loading Versus  
Voltage Silver



MU-4355

Fig. 38 - X-Ray Loading Versus  
 Voltage OFHC Copper



MU-4356 7

Fig. 39 - Variation of Sparking Rate  
with Electrode Temperature



Fig. 40 - Spark crater .025 in. in diameter. Inconel Electrodes. Note .002 - .008 in. radial cracks.



Fig. 41 - Extensive recrystallization .005 to .007 in. into the surface of Inconel electrodes.



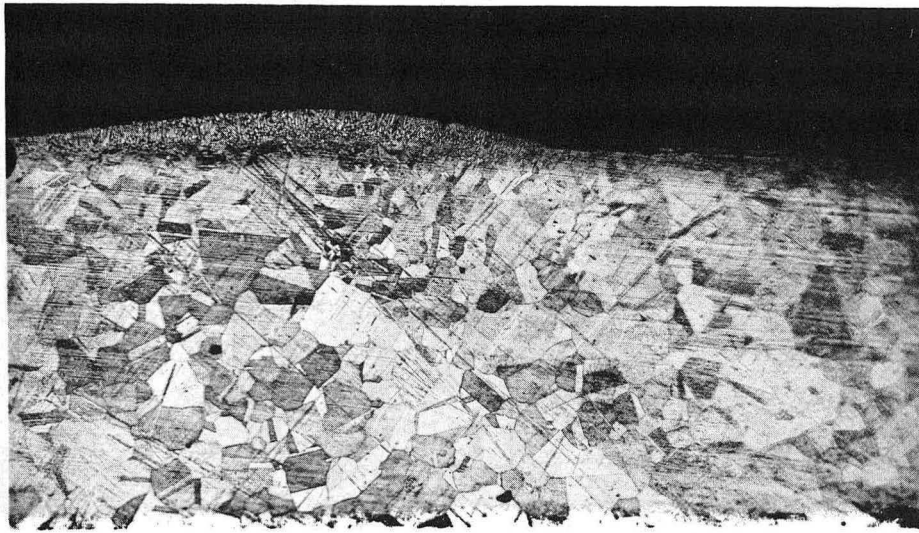


Fig. 42 - Fusile bond of material transferred across the gap as a result of a spark. Inconel.



Fig. 43 - Mechanical bond of material transferred across the gap as a result of a spark. Inconel.

